Li, S, Li, L, Tu, H, Zhang, H, Silvester, DS, Banks, CE, Zou, G, Hou, H and Ji, X (2021) The development of carbon dots: From the perspective of materials chemistry. Materials Today, 51. pp. 188-207. ISSN 1369-7021

DOI: https://doi.org/10.1016/j.mattod.2021.07.028

Publisher: Elsevier

Version: Accepted Version

The development of carbon dots: From the perspective of materials chemistry

Shuo Li [a], Lin Li [a], Hanyu Tu [a], Hao Zhang [a], Debbie S. Silvester [b], Craig E. Banks [c], Guoqiang Zou [a], Hongshuai Hou [a,⇑], Xiaobo Ji [a,d]

[a]State Key Laboratory of Powder Metallurgy, College of Chemistry and Chemical Engineering, Central South University Changsha, 410083, China
[b] School of Molecular and Life Sciences, Curtin University, GPO Box U1987, Perth, Western Australia 6845, Australia
[c] Division of Chemistry and Environmental Science, Manchester Metropolitan University, Manchester, M1 5GD, UK
[d] School of Materials and Engineering, Zhengzhou University, Zhengzhou, 450001, China

The advance of materials chemistry has influenced significantly the lifestyle of mankind. By virtue of their fascinating physicochemical nature – including ultrasmall size (<10 nm), rich functional groups, fluorescence, chemical stability, biocompatibility, and nontoxicity – carbon dots have been acclaimed as another epoch-making carbon-based nanomaterial following on from fullerene, nanotubes, and graphene. However, the field of carbon dot-based materials chemistry remains incomplete because of their wide structural diversity, meaning that much fundamental knowledge still needs to be uncovered. Herein, this review proposed several novel viewpoints in term of carbon dot-based material chemistry, including the development history, classification, design principle and applications of carbon dots-based materials. Finally, several sound prospects in this fascinating filed are also given.

Keywords: Carbon dots; Carbon quantum dots; Graphene quantum dots; Carbon dot-based composite; Materials chemistry

Introduction

Many revolutionary progress of mankind is closely associated with evolution of materials chemistry [1]. Carbon-based nano-materials, such as fullerene [2], carbon nanotubes [3], graphene [4], and their derivatives [5,6] have been successively proven as sound materials and given rise to a booming of a variety of appli-cations. As an emerging member of the “carbon family”, carbon dots (CDs) – typically defined as small carbon nanoparticles with size less than 10 nm – are becoming a hot topic in materials chemistry thanks to their combination of superior properties [7]. In our opinion, the evolution of carbon dot-based materials chemistry involves three distinct stages (Fig. 1a): (Ⅰ) the discovery stage of CDs (2004–2006), (Ⅱ) the initially developing stage of CDs (2007–2011), and (III) the explosively developing stage of CDs (2011-now). More specifically, stage (Ⅰ) refers to the initial time when CDs were named and defined.

Historically, the significant scientific discoveries were always serendipitous. CDs was first reported and described as “fluores-cent nanoparticles” by Xu et al. [8] in 2004 during the purifica-tion of single-walled carbon nanotubes through preparative electrophoresis. However, the wide interest of researchers was not stimulated in this field until the term “carbon quantum dots” was defined formally by Sun et al. [9] in 2006. The term “carbon dots” is utilized to precisely distinguish them from the much broader field of carbon nanoparticles, such as carbon black [10]. Since then, studies on the properties of CDs were reported sporadically, but the fundamental knowledge about CDs remained elusive.

In stage (Ⅱ), major existing fabrication strategies were explored using carbon-containing materials as precursors to gen-erate CDs (Fig. 1b). Interestingly, it was found that the optical and electrochemical properties of CDs can occur by varying the experimental parameters, and thus the interest of scholars towards the structure–property relationship of CDs was widely stimulated. In addition, the potential application of CDs in

---

⇑ Corresponding author.
E-mail address: Hou, H. (hs-hou@csu.edu.cn)

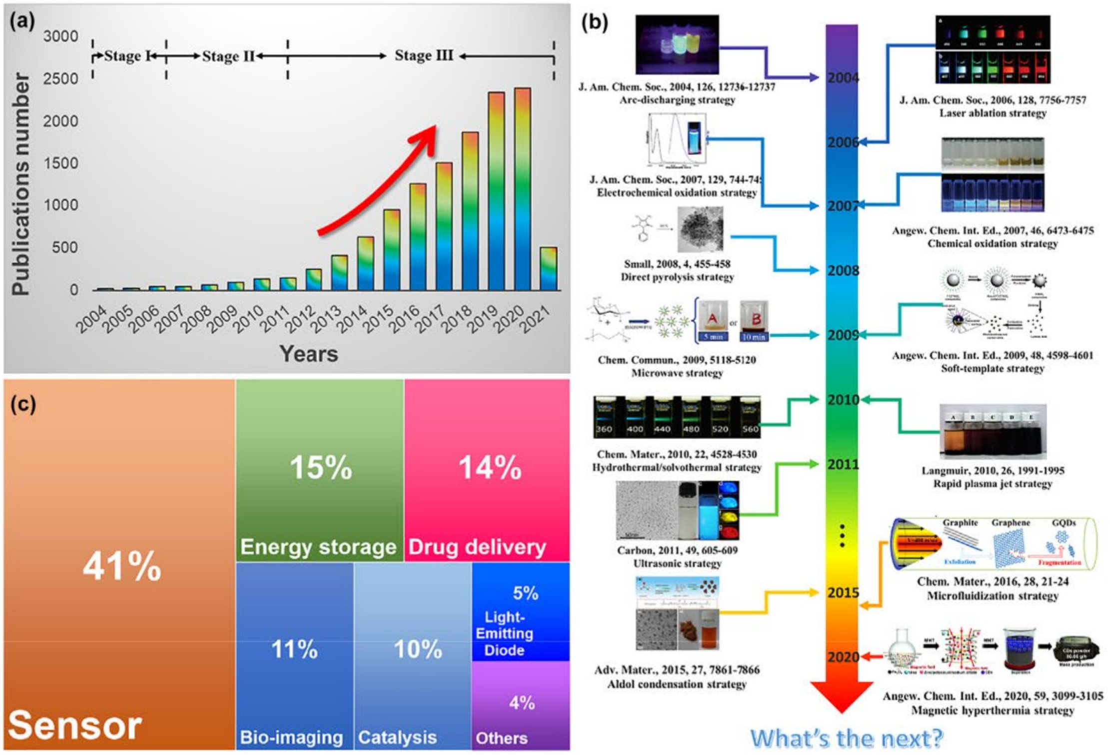

FIGURE 1

The evolution process of CD-based materials chemistry. (a) The histogram depicts the number of publications on CDs from 2004 to 2021 obtained from ISI Web of Science in March 2021. (b) The timeline shows progress on the fabrication strategies of CDs. Reproduced with permission [8,9,11,24,75,120,127,131– 133,139,143]. Copyright 2009 Royal Society of Chemistry, 2007, 2008, 2009, 2015 and 2020 Wiley-VCH, 2004, 2006, 2007, 2010 and 2016 American Chemical Society, 2011 Elsevier Ltd. (c) A schematic depicting the proportion of publications on CDs in various applications from 2004 to 2021 obtained from ISI Web of Science on March, 2021.

various filed began to gain more and more attention as well [7], which demonstrated major impact in the following development of carbon dot-based materials chemistry.

In stage (III), there was an exponentially increasing number of publications about CDs since around 2011 (Fig. 1a), when the practicality of CDs was starting to be considered frequently. Apart from the expansion of their application scope, a series of large-scale synthetic strategies of CDs were reported for reducing the cost of making the CDs [11,12].

As analogues to semiconductor quantum dots, CDs can give rise to tunable photoluminescence (PL) induced by various fac-tors (as will be further discussed later) [10,13]. In addition, CDs possess the superior merits of carbon nanomaterials as well, such as low toxicity, ultrahigh specific surface area, chemical inert-ness, excellent electron-transfer properties. Hitherto, CDs are widely regarded as a highly promising nanomaterial and their impact in multiple different applications has been demonstrated (Fig. 1c). These include applications in sensor [14], energy storage [15], drug delivery [16,17], bio-imaging [18,19], catalysis [20,21] and light-emitting diode (LED) fields [22,23]. Thus, it is necessary to consider CDs in the realm of materials chemistry.

Nevertheless, the area of CDs-based material chemistry remains not fully-complete, and many fundamental knowledge needs to be further investigated, including the nature and mod-ification of CDs, the effect and mechanism of CDs in materials synthesis and applications. Just as the proverb says, “If you can't measure it, you can't manage it”. Herein, this review will address several new viewpoints in terms of CDs-based materials chemistry, highlighting the latest progress in this field. We indeed hope that this review can give better guidance into designing the ideal CDs and their nanohybrids.

Classification of CDs

“Carbon dots” are hard to define and classify accurately by virtue of their diversity of nanostructure. In some early literature, car-bon dots were loosely defined as “fluorescent nanoparticles” [8] and “carbogenic dots” [24]. Herein, based on various previous works [25–27], we suggest that CDs can be divided mainly into five categories according to the diversity of carbon core: (1) gra-phene quantum dots, (2) graphitic carbon nitride quantum dots, (3) carbon quantum dots, (4) carbon nanodots, and (5) car-bonized polymer dots (Fig. 2a).

Graphene quantum dots

Graphene quantum dots (GQDs), strictly speaking, are defined as single-layer graphene with a diameter of less than 10 nm. How-ever, in practice, GQDs are present with a few atomic layers con-taining functional groups on the edges or inner layer defects due to their non-ideal preparation conditions [25,26,28]. The thick-ness of GQDs can significantly alter their physicochemical prop-erties (e.g., absorbance) [29]. Additionally, as the graphitic fragment, GQDs exhibit reserved graphitic domains (sp^2 domains) and have similar graphitic in-plane lattice spacing

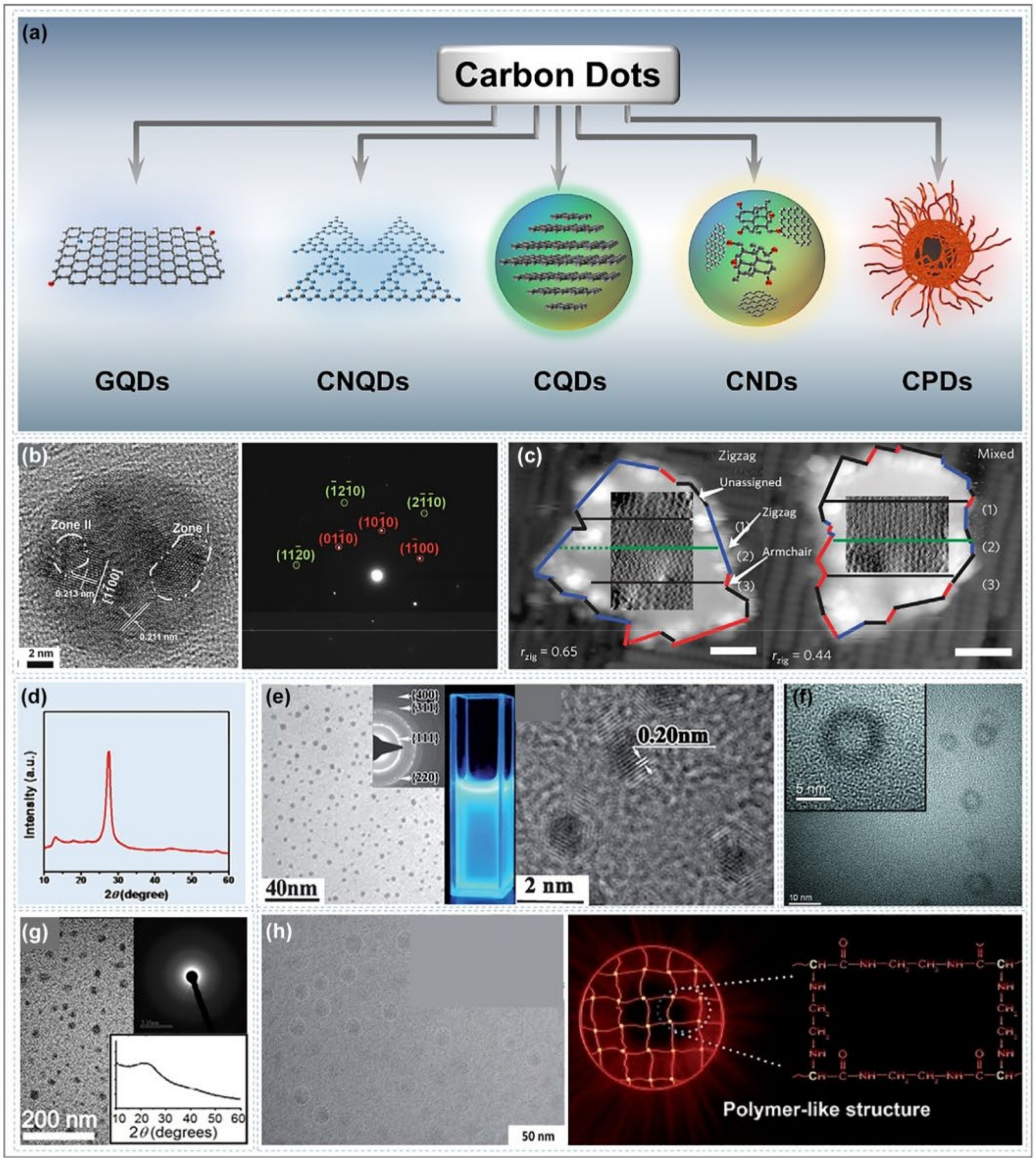

FIGURE 2

The classification of CDs. (a) Schematic depicting the nanostructure of various CDs. (b) The TEM image (left) and corresponding SAED image (right) of GQDs. Reproduced with permission [30]. Copyright 2014 Wiley-VCH. (c) The spatially resolved tunnelling spectroscopy image of zigzag- (left) and mixed-edge GQD (right). Reproduced with permission [32]. Copyright 2009 Nature Publishing Group. (d) The XRD pattern of CNQDs. Reproduced with permission [37]. Copyright 2013 Royal Society of Chemistry. (e) The TEM image (left), the corresponding SAED image (insert) as well as their HRTEM image (right) of CQDs. Reproduced with permission [43]. Copyright 2009 Royal Society of Chemistry. (f) The TEM and its magnification image (inset) of hollow CQDs. Reproduced with permission [16]. Copyright 2013 Elsevier Ltd. (g) The TEM image and corresponding SAED image (inset 1) as well as XRD pattern (inset 2) of CNDs. Reproduced with permission [46]. Copyright 2018 Nature Publishing Group. (h) The TEM image of PDs (left) and the schematic depicting their carbon core. Reproduced with permission [48]. Copyright 2017 Wiley-VCH.

(0.18–0.24 nm, corresponding to different diffraction planes) and graphitic inter-layer spacing (0.334 nm) as bulk graphite (Fig. 2b) [28,30], albeit with the fact that graphite lattice spacing can be varied via doping of heteroatoms to match application demands [31]. Furthermore, the edge site of GQDs contributes their predominant properties and has a non-negligible role for their performance, namely “edge effect” (Fig. 2c) [32] (as will be further discussed later).

Graphitic carbon nitride quantum dots

The graphitic carbon nitride quantum dots (g-CNQDs) with graphene-like 2D structure are generally regarded as analogues of GQDs, and thus are rarely discussed individually. But this view should be corrected due to their significantly different element content and nanostructure [33]. Actually, carbon nitrides have several allotropes – and there are even reports about C_3N quantum dots [34] – but graphitic carbon nitride (g-C_3N_4) is outstanding thanks to its more stable nanostructure in ambient environments [35]. Similar to 2D g-C_3N_4 sheet, g-CNQDs consist of tri-s-triazine units bridged by amino groups, with periodic vacancies in their lattices [36]. The unique ‘poly(tri-s-triazine)” framework with highly defective and abundant amine groups (–NH or –NH_2) on the terminating edges impart g-CNQDs excel-lent catalytic and other properties [33]. Zhang et al. [37] prepared g-CNQDs with high crystallinity and a lattice parameter of 0.34 nm, which corresponds to the two characteristic peaks at 27.41 and 13.11 in the XRD pattern, respectively (Fig. 2d). Li et al. [38] reported g-CNQDs modified by phenyl groups through supramolecular preorganization, which significantly altered the p-electron delocalization in the conjugated g-C_3N_4 networks. Li et al. [39] proposed that g-C_3N_4 with large size showed poor absorbance of visible-light to generate photoelectrons, which could be ascribed to the diminished quantum size effect similar to GQDs. To date, there are fewer reports about the preparation and application of g-CNQDs than that of GQDs, but the prospect of CNQDs is good in the future thanks of their sound nature.

Carbon quantum dots

In terms of carbon quantum dots (CQDs), the mainstream views suggest that they feature quasi-spherical carbonic nanoparticles which exhibit a crystalline core based on a mixture of sp^2 and sp^3 carbons [13,40]. For instance, Qu et al. [41] proposed supra-(carbon nanodots) with non-uniform lattice fringes (d_{100} = 0.21 nm) between adjacent locations. The high carbon-lattice-structure content was further indicated by the Raman spectrum, in which the relative intensity of the D band and G band (I_D/I_G = 0.87). Pang et al. [42] suggested that their CQDs rendered the lattice spacing ca. 3.25 Å, corresponding to the

(2) facet of graphite. Du et al. [43] reported that CNDs exhib-ited a diamond-like structure by means of selected area electron diffraction (SAED) pattern and HRTEM (Fig. 2e). In addition, their high specific surface area is also an attractive feature for researchers. For example, Zheng et al. [16] reported novel hollow carbon dots (HCDs) as shown in Fig. 2f, which presented a sur-

face area of 16.4 m^2 g ^{1}, pore volume of 1.73 10 ^{2} cm^3 g ^{1} as well as an average simulated pore diameter of 2.2 nm based on the Barrett–Joyner–Halenda (BJH) model.

Carbon nanodots

The term “carbon quantum dots” and “carbon nanodots” were often confused in some reports. Some researchers claimed that carbon nanodots (CNDs) refers to quasi-spherical carbonic nanoparticles which mainly consist of an amorphous structural core, unlike the CQDs [44,45]. For instance, Ray et al. [46] pre-pared CNDs without a distinct crystal lattice, which is shown by the broad hump centered around ~ 2h = 26L in the X-ray diffraction profile (Fig. 2g). Although only little has been explored so far, their luminescence properties and relatively low cost enable CNDs to be applied in the future. I think it is not of scientific significance to distinguish carbon nanodots and carbon quantum dots according to the crystal structure of carbon core, but only for artificial classification. Both of them can be used to describe the spherical CDs.

Carbonized polymer dots

The term “carbonized polymer dots (CPDs)” involves carbonic nanoparticles derived from the aggregation or cross-linking of linear polymers or monomers, which is significantly different from aforementioned CDs [25]. Their carbonized core con-tributes the predominant properties (e.g., enhanced fluorescence [47]) of CPDs compared with traditional polymer dots. Yang et al. [27] suggested that the carbon core of CPDs included sev-eral subcategories: complete carbonized cores, the paracrystalline carbon structure composed of tiny carbon clusters with polymer frameworks, as well as the highly dehydrated crosslinking and curling polymer framework. The degree of carbonization of CPDs is highly dependent on the reaction parameters and nature of the precursor. For instance, Yang et al. [48] prepared novel CPDs based on maleic acid (MA) and ethylenediamine (EDA). The con-densation polymer was further crosslinked, resulting in the inner polymer core with network structure (Fig. 2h). Likewise, many studies suggest that PDs based on polymerization of organic molecules (e.g., acetone [11], acetaldehyde [49], polythiophene phenylpropionic acid [50]) can also generate CPDs with a close-knit polymer structure core. CPDs can also be obtained via modifying other CDs with polymer molecules [9]. CPDs gen-erally possess highly stability towards pH, ionic strength, and UV exposure owing to their crosslinked structure, showing great potential as a material for use in various applications, especially for vivo drug/gene/protein delivery systems [51].

Design of CDs

Design principle of CDs

Various properties of CDs can be imparted by regulating the microstructure of CDs. The quantum size is the most significant feature of CDs, which is highly dependent on the synthetic pro-cess (e.g., the ratio of precursor [52], reaction time [23], temper-ature [53], solvent [54] and so on [55]). This part will be further discussed in Section “Fabrication of CDs”. On the other hand, various strategies aiming to modify the surface state of CDs have been presented since Sun et al. [9] firstly reported an optimiza-tion strategy of CDs. The modifying strategies can be divided into three categories, that is, heteroatoms doping, surface func-tionalization and surface passivation. Heteroatom doping is a common method in the preparation of CDs, where other ele-ments (e.g., N, B, S, P and halogen) are used as a dopant to replace carbon atoms in the sp^2/sp^3 network [56]. Surface functionalization is generally related with covalently bonded func-tional groups (containing O and H that saturate the dangling bonds in N, S, B etc.) on carbon basal surfaces or edge planes [56]. Surface passivation means that passivating regents (e.g., polyethylene glycol (PEG) [9]) are coated on the surface of the carbon core of CDs to regulate their surface state [57]. In general, the size and surface state of CDs have a direct impact on their energy gap, thereby causing a change in their performance. Therefore, it is meaningful to explore the origin of the energy gap of CDs.

Currently, the generally accepted view of controlling the energy gap between the highest occupied molecular orbital (HOMO) and the lowest unoccupied molecular orbital (LUMO) of CDs can be summarized with the quantum confinement effect and the surface energy trap mechanism [58]. The quantum con-finement effect means that graphene fragments have a non-zero bandgap because of excitons in graphene with an infinite Bohr diameter [26]. In terms of quantum confinement effect, there are two major origins of conjugated-domains and the edge site that needs to be considered [59]. As for CDs with a perfect gra-phene core and fewer surface chemical groups, increasing the size of conjugated-domains leads to a narrowing of the energy gap [60]. For instance, Kang et al. [61] purified and isolated CDs with different sized domains through simple column chro-matography. Analysis suggested that the energy gap of CDs decreased gradually while the sp^2 domain size of CDs increases. Chhowalla et al. [62] regulated the sp^2-domain size through decreasing the carbon–oxygen sp^3-domain of GQDs and saw sim-ilar results (Fig. 3a). In addition, the edge site can also influence significantly for the energy gap of CDs. For example, Chen et al. [63] proposed that zig-zag-edged GQDs exhibited a lower energy gap than their armchair-edged counterparts due to the localized states on the zigzag edges.

The surface energy traps highlight the role of the surface state on the energy gap of CDs. In practice, CDs consist of numerous carbonaceous sp^2 and sp^3 domains, which are accompanied by various defects with non-perfect sp^2 domains, and thus exhibit multiple electron transitions between energy gaps. Pang et al. [64] reported that surface defects induced by surface oxidation can serve as capture centers for excitons, causing a narrow band gap for CDs. Xiong et al. [18] generated a series of CDs with broad size distributions but different surface states. Their results suggested that the band gap between the LUMO and the HOMO reduced with increasing oxidation amounts on CD surfaces (Fig. 3b). The role of surface oxidation was further discussed by Yeh et al. [59]. More specially, incorporating oxygen atoms into the sp^2-domain induced the emergence of the n-orbital level, thereby resulting in the generation of n-p* transition of electrons (Fig. 3c). Generally, incorporating heteroatoms with high elec-tronegativity values (e.g., nitrogen, sulfur and phosphorus) into the sp^2-domain can narrow their band gap [65,66].

In addition, the nitrogen-containing functional groups are quite popular among surface functionalization and passivation of CDs. For instance, Tetsuka et al. [67] incorporated different nitrogen-containing functional groups with varying degrees, which changed the HOMO/ LUMO energy levels of CDs,

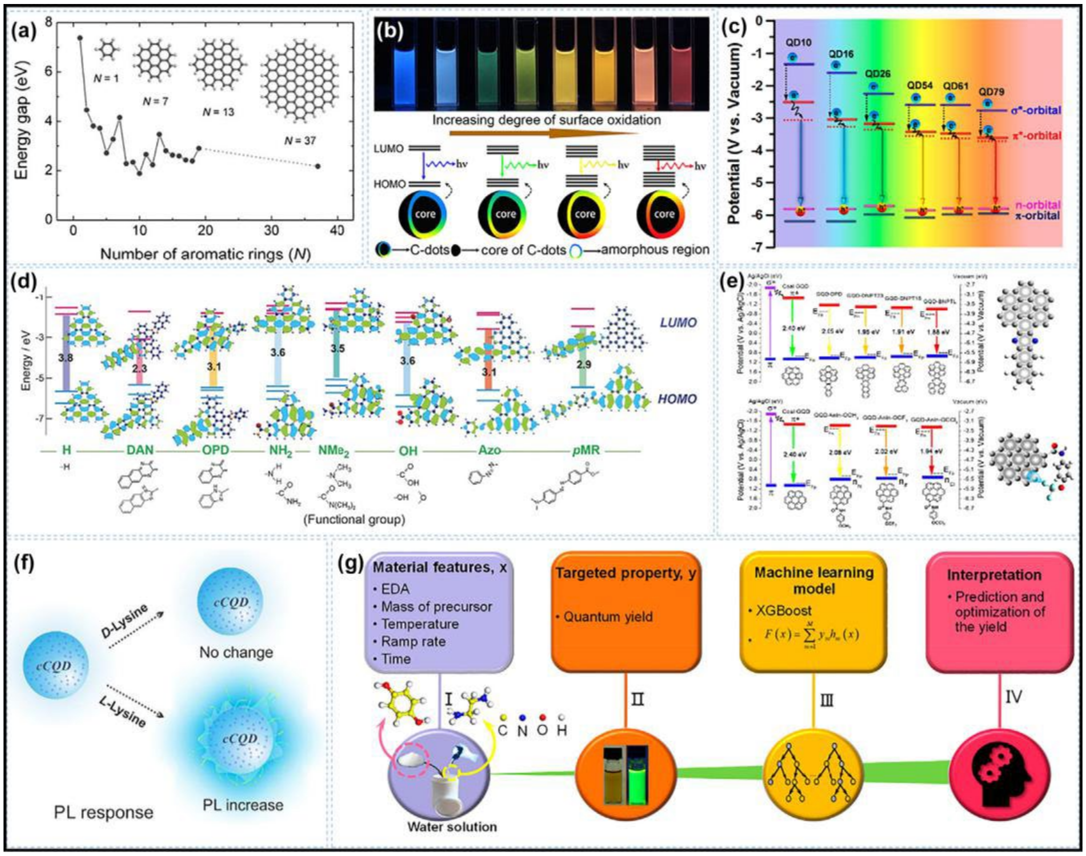

FIGURE 3

The design principle of CDs. (a) Interrelation of the energy gap with the number of fused aromatic rings (N) of GO. Reproduced with permission [62]. Copyright 2010 Wiley-VCH. (b) Schematic depicting the energy gap of CDs with different degrees of oxidation. Reproduced with permission [18]. Copyright 2016 American Chemical Society. (c) Schematic depicting the effect of incorporating oxygen atoms on the energy gap of CDs. Reproduced with permission [59]. Copyright 2016 American Chemical Society. (d) Schematic depicting the effect of incorporating nitrogen-containing functional group on the energy gap of CDs. Reproduced with permission [67]. Copyright 2016 Wiley-VCH. (e) Schematic depicting the effect of incorporating electron-donating fictional group or increasing sp^2 domain size on the energy gap of CDs. Reproduced with permission [68]. Copyright 2017 American Chemical Society. (f) The schematic depicting the PL performance of CDs after L- and D-lysine modifying. Reproduced with permission [71]. Copyright 2019 Elsevier Ltd. (g) The schematic depicting the design framework of machine learning driven synthesis of CDs. Reproduced with permission [74]. Copyright 2020 American Chemical Society.

resulting from the strong orbital interactions (Fig. 3d). More specifically, the functional group of o-phenylenediamine, diaminonaphthalene, azo, and p-methyl red led to lower energy levels, whereas NH$_2$ or dimethyl amine resulted in degenerate HOMO orbitals and higher energy levels. Recently, Chen et al. [68] reported that the bandgap of CDs can be narrowed through offering an electron-donating functional group on the surface of CDs, which could introduce n-orbital between p and p* orbitals (Fig. 3e). They proposed that the effect could be achieved by con-jugating CDs with poly-aromatic rings to enlarge the p-conjugated sp^2-domain. The role of other functional groups has been reported as well [22].

Surface passivation with a polymer molecule is another effi-cient strategy to alter the performance of CDs. For example, Sun et al. [9] passivated CDs with diamine-terminated oligomeric poly-(ethylene glycol) (PEG$_{1500N}$) to boost the fluorescence emis-sions of CDs. The surface passivation is beneficial for removing the surface dangling bonds, which is apt to prefer the trapping of electrons through a non-radiative pathway. Meanwhile, one has to keep in mind that this strategy is cumbersome, strongly cytotoxic and environmentally toxic by virtue of hazardous passivation agents [65].

The chirality of CDs is becoming another hot topic in the design of CDs, because chirality significantly influences the physicochemical properties of CDs. The chirality of CDs can be imparted via chiral synthesis or chiral assembly [69]. The former involves a chiral molecule (typically using amino acid enan-tiomers [70]) as precursor for generating CDs modified by chiral ligand (Fig. 3f) [71], whereas the latter involves arranging CDs by means of a chiral matrix [72]. Compared to normal CDs, chiral CDs generally exhibit excellent chemical stability, in addition to improved electronic and optical performance due to their unique nanostructure [69]. What’s more, the chirality of CDs can be transferred while combining them with other molecules [73] making chiral CDs fascinating in various fields such as med-icine [70].

To avoid numerous trial and error processes, a series of com-putational models based on quantum chemistry have been pro-posed [22,74]. Designing CDs by means of artificial intelligence technology might be a promising research direction. For instance, Wu et al. [74] recently proposed a novel “machine learning driven synthesis” of CDs, in which the corresponding relationship between various reaction factors and the quantum yield of CDs was quantitatively analyzed using artificial intelli-gence (Fig. 3g). Thus, the optimum conditions for the prepara-tion of CDs can be predicted and identified via only a few trial-and-error processes.

Properties of CDs

Optical properties

Due to the quantum-confinement effect, the optical properties are the most notable commonalities of CDs even though they are very diverse in terms of nanostructure. CDs generally render strong absorption in the near ultraviolet region (230–270 nm) induced by electronic transitions from p to p* of the phenyl rings [75], whereas lower absorption intensity in the visible and near infrared (NIR) region is induced by the n-p* transition of C@C or C@O bonds [76]. The curve shape and intensities can be changed by heteroatom doping as well as surface modification [77,78].

Once excited by the absorption of light, the unique tunable photoluminescence (PL) contributes the predominant feature of CDs to be applied in various applications [26,79]. The major PL mechanism of CDs consists of (1) the quantum confinement effect mechanism [61], (2) the surface state mechanism [18,80], (3) the molecule state mechanism [53], and (4) the crosslink enhanced emission (CEE) effect mechanism [26]. For mechanisms (1) and (2), it is noticeable that the emission wavelength of CDs increases with their band gap narrowing, which has been discussed in Sec-tion “Design principle of CDs”. The molecule state mechanism means that the PL of CDs is imparted directly by an organic fluo-rophore on their surface rather than their chemical groups or car-bon core [26]. It should be noted that this mechanism applies only to the CDs generated at a moderate heating temperature because of the emergence carbogenic aggregation and decomposition of molecular fluorophores at high temperature [53] (Fig. 4a). As for the CEE effect mechanism, it was firstly proposed by Yang et al. [47] to describe the PL performance of non-conjugated CPDs. More specifically, the rotation and vibration of the sub-fluorophore on the CPD surface can be efficiently immobilized in the presence of the crosslinking skeleton and/or carbon core, resulting in a boosted radiative transition (Fig. 4b).

The research interests for up-conversion and phosphores-cence of CDs have surged recently [81,82,83,84]. Up-conversion, which is multiphoton absorption or anti-stokes photoluminescence, means that CDs emit a higher frequency photon after absorbing two or more photons of lower frequency, which is promising for in-vivo bioimaging since bioimaging at longer wavelengths is usually preferred. Sun et al. [83] first dis-covered the up-conversion phenomenon of CDs and demon-strated the potential of CDs for cell imaging in 2007. Subsequently, Kang et al. [61] prepared CDs with narrow size dis-tribution and further observed that up-converted PL of CDs located in the range from 325 to 425 nm under an long excita-tion wavelength from 500 to 1000 nm (Fig. 4 c).

What’s more, the unique phosphorescence nature, which is one of the most characteristic delayed-luminescence subtypes, enables CDs to be applied in several specific fields, especially in anti-counterfeiting [85]. Generally, the phosphorescence perfor-mance can be only observed at ultralow temperatures, which can be ascribed to the fact that phosphorescence is hindered by the spin-forbidden nature of triplet exciton transitions and non-radiative decay processes [86]. Recently, Jiang at el. [82] suggested that CDs with room temperature phosphorescence (RTP) could be obtained directly if their structure met following principles:

(1) an amorphous polymer-like nanostructure that serves as a matrix to embed and immobilize luminogens; (2) contain surface functional groups that could generate hydrogen bonds, and (3) doping heteroatoms that favor the n–p* transition (e. g., N, P and halogens). Based on this, CDs with ultralong RTP lifespan (~1.46 s) was obtained (Fig. 4 d) and showed promising potential in anti-counterfeiting. The phosphorescence behavior of CDs in aqueous solution was reported by Zhou et al. [87]. Analysis showed that cyanuric acid (CA) and CDs enable the construction of hydrogen-bonded networks in water, resulting in the stabiliza-tion of the excited triplet species.

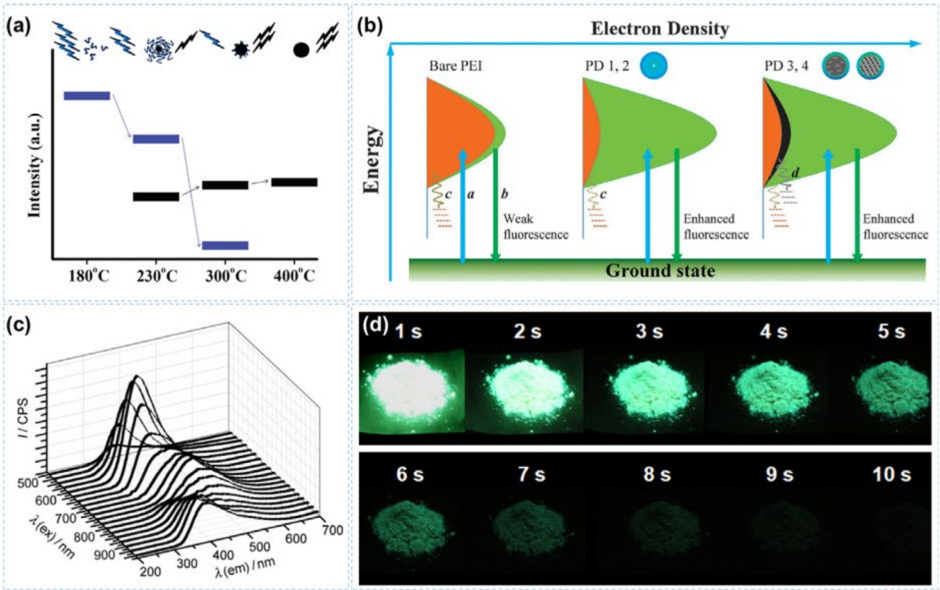

FIGURE 4

The fluorescent nature of CDs. (a) Schematic depicting the PL intensity aroused from a carbon core (black bar) and organic fluorophores (blue bar) at different carbonization temperatures. Reproduced with permission [53]. Copyright 2012 American Chemical Society. (b) Schematic depicting the CEE effect mechanism of a bare PEI and corresponding PDs. Reproduced with permission [47]. Copyright 2014 Royal Society of Chemistry. (c) The up-conversion PL nature of CDs. Reproduced with permission [61]. Copyright 2010 Wiley-VCH. (d) A digital photo of the RTP phenomenon of CDs after ceasing the UV lamp (365 nm). Reproduced with permission [82]. Copyright 2018 Wiley-VCH.

Electrochemical properties

The electrochemical properties of CDs play a key role in various applications, because they are highly correlated with their car-bon core and surface state [88,89]. The electrochemical proper-ties of CDs are mainly influenced by the quantum confinement effect and the surface energy trap, which is significantly distinct with a 2D graphene layer [58,63]. CDs can play a role as electron acceptors and electron donors for various applications, in which electrons and holes emerge and are then transferred to other spe-cies after exciting by photons. Hitherto, many efforts have been undertaken to explore the relationship between their electronic properties and carbon core. For instance, Pillai et al. [90] pre-sented that the size of GQDs has a demonstrated impact on entrapping single electrons between the GQD and their surface. Chang et al. [91] suggested the energy gaps of GQDs can be reg-ulated by altering the electric field, which can be ascribed to the spatial anisotropy of GQDs. Likewise, Ritter et al. [32] succeeded in observing the different edge configurations of GQDs by means of tunneling spectroscopy, and showed the presence of zig-zag edge states predominantly due to the fact that the zig-zag-edged GQDs were metallic. As for amorphous CDs with poor electrochemical performance, Dirk M. et al. [44] suggested it might be ascribed to the elemental composition and the number of sp^{3}-carbon atoms having a weaker impact on the electronic structure of amorphous CND compared to that of an sp^{2}-network.

Compared to designing the carbon core, heteroatom doping and surface functionalization may be more effective strategies to optimize the electrochemical performance of CDs. In terms of electron transfer, in principle, incorporation of electron-donating heteroatoms (e.g., nitrogen) can lead to a faster rate of heterogeneous electron transfer (HET), whereas doping with electron-withdrawing heteroatoms (e.g., halogens) exhibits decreasing HET rates [88]. The presence of a higher amount of oxygen functional groups on CDs can lead to slower electron transfer as well, due to disruption of the conductive sp^{2} carbon network [28]. More and more studies tend to explore the influ-ence of dual-/multi-element co-doping towards electron transfer of CDs by virtue of their excellent cooperative effect. Metal dopants can significantly boost charge transfer of CDs as well. For instance, Wu et al. [92] proposed that the high electric con-ductivity (171.8 ls cm ^{1}) of CDs was achieved through doping with a copper (Cu) atom. The Cu (II) ions and functional groups of CDs can generate a Cu–ligand bond and thus optimize charge transfer inside CDs, significantly boosting the electron-accepting (2.5 times) and -donating abilities (1.5 times) compared to that of CDs without incorporated Cu.

The electron transfer from CDs results in the emergence of fluorescence resonance energy transfer (FRET). The term “FRET” encompasses the interaction of two fluorescent components that are at a distance typically on the order of 10 nm. Energy transfer from a donor (with higher energy) to an acceptor (with lower energy) occurs, boosting the fluorescence of the acceptor but sac-rificing the fluorescence or quenching of the donor [93]. This phenomenon is a working foundation for the application of CDs in the sensors field. Many efforts have also been taken to avoid fluorescence quenching. For instance, Lu et al. [94] achieved solid-state fluorescent CDs via doping with boron atoms, which can generate electronic defects that inhibit the charge transfer. Naturally fluorescence quenching of CDs also can be inhibited through combining with materials, such as poly(vinylalcohol) [95], and starch [96] in a matrix.

Dispersibility

It is necessary to consider the role of dispersibility of CDs, as this significantly influences the application of CDs. In some reports, CDs were called “water-soluble CDs” [97] or “oil-soluble CDs” [98]. But these terms are inaccurate because CDs in solution exist actually in the form of colloids, thereby resulting in the emer-gence of the “Tyndall effect”. Zhu et al. [99] divided CDs into three types: hydrophilic, hydrophobic and amphiphilic, accord-ing to their distinct “solubility” in aqueous and/or organic sol-vents (Fig. 5a). The surface state of CDs plays a non-negligible role in regulating their dispersibility [77]. CDs are apt to be hydrophilic when their surface mainly consists of hydrophilic functional groups (e.g., –OH, –COOH). Thus, most CDs are well hydrophilic in nature owing to introduced oxygenated function-alities during their preparation process.

The research interest of hydrophobic carbon dots has surged in some applications recently, such as their application as an organic electrolyte additive [100]. For instance, our group [49] found that CDs prepared form acetaldehyde or acetone as a car-bon source exhibited excellent dispersibility in various organic solvents (e.g., ethanol, acetone, benzyl alcohol, tetrahydrofuran, dimethyl formamide, 1-methyl-2-pyrrolidinone, dimethyl sul-foxide, and propylene carbonate) (Fig. 5 b). The ideal dispersibil-ity in organic solvents can be ascribed to the stretching and bending vibrations of the carbon-hydrogen single bond (C–H) in the methyl groups [101]. Hydrophobic carbon dots can be obtained from surface passivated hydrophobic molecules as well. Pan et al. [102] succeeded in preparing hydrophobic carbon nanoparticles using dodecylamine (DDA) as a passivated agent, which covalently linked with the –COOH group on the surface of the pre-prepared carbon nanoparticles.

As mentioned above, the fluorescent quenching effect emerges when CDs are aggregated, which seemingly suggests that the dispersibility of CDs is a key factor for their fluorescence performance. Very recently, Yang et al. [103] observed the abnor-mal (but reversible) red-shift behavior when hydrophobic CDs were added into water and further aggregated (Fig. 5c). This on–off fluorescence might be ascribed to the dominant surface energy transition of CDs. Additionally, Wang et al. [104] pre-pared amphiphilic CDs using p-Phenylenediamine and diphenyl ether as precursors. The presence of hydrophilic and hydropho-bic functionalities imparted good dispersibility of the prepared CDs in both of water and organic solvents (CCl_4, toluene, $CHCl_3$, acetone, DMF, CH_3OH). Interestingly, the emission peaks of the CDs solution red-shifted from 511 to 615 with an increasing of the solvent polarity, which was attributed to the formation of strong hydrogen bonds between the CDs and solvent molecules.

Toxicity

“Low toxicity” has been regarded as one of the most significant superiority of CDs compared to semiconductor quantum dots, which imparts their potential for bio-imaging as well as their use in nanoscale dimensions [28]. Numerous studies suggest that CDs render non-negligible cytotoxicity to various cell lines (e.g., Hela cells [50], human breast cancer cell [105], madindarby canine kidney epithelial cells [106]) at moderate concentration levels. But it should be noted that the term “low” is very loosely. Over an optimum concentration, CDs will actually lead to the emergence of shrinkage and holes on the surface of cells, result-ing in less growth of the cell in vivo/vitro [107]. Besides, the tox-icity of CDs can be altered by external solutions as well. Cytotoxicity studies are generally carried out in the dark, which

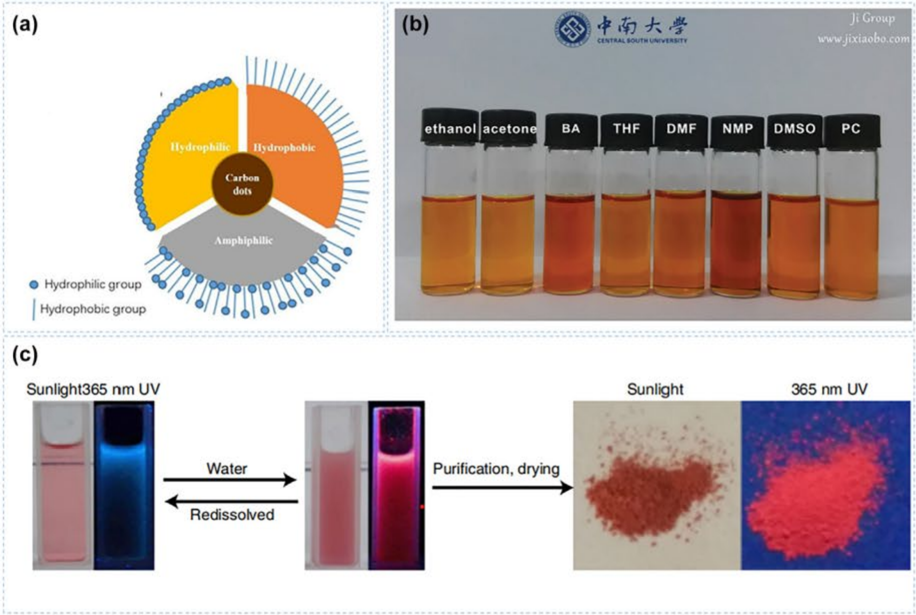

FIGURE 5

The dispersibility of CDs. (a) Schematic depicting the different surface states of hydrophilic, hydrophobic and amphiphilic CDs. Reproduced with permission [99]. Copyright 2018 Royal Society of Chemistry. (b) A digital photo of hydrophobic CDs in various organic solvents. Reproduced with permission [49]. Copyright 2017 Wiley-VCH. (c) A digital photo of CDs with red aggregation-induced emission and their solutions. Reproduced with permission [103]. Copyright 2019 Nature Publishing Group.

is a discrepancy with their practical application (e.g., bioimaging) [19]. With adequate studies on the toxicity, however, there are growing signs that light-irradiated CDs might be toxic to bacteria or cells due to the emergence of reactive oxygen species. Very recently, Miao et al. [108] presented that the photodegradation phenswomenon was ubiquitous for CDs, and will further aggra-vate photo-induced production of CD radicals (e.g. hydroxyl and alkyl radicals). Analysis suggested that higher temperature, higher pH, more light intensity and shorter wavelengths will induce more rapid photodegradation of CDs.

Fabrication of CDs

The fabrication strategy of materials is one of the most important considerations in the subject of materials chemistry. The diverse morphology of CDs are closely associated with various synthetic methods and precursor [10]. The synthetic strategies of CDs can be mainly divided into two types, that is, “top-down” and “bottom-up” strategies [26] (Fig. 6a and Table 1). The “top-down” strategies refer to “breaking down” carbon target, includ-ing grapheme [109], graphitic carbon nitride [37], fullerenes [110], coke [111] and Super P [112] under harsh reaction condi-tions. This strategy is popular for the generation of GQDs and CNQDs, and thus their plane structure is inherited from their precursor. The “bottom-up” strategies, however, involves poly-merization and carbonization of small molecule precursors, such as citric acid [113,114], glucose [115], acetaldehyde [116], and phenylenediamine [18]. In general, other CDs (e.g., CQDs, CNDs, CPDs), which exhibit lower carbonization degree of car-bon core than that of GQDs, are obtained for this type strategies.

Top-down strategies

Arc-discharging and laser ablation of a bulk carbon-based target (e.g. activated carbon [117] and oriented pyrolytic graphite [118]) were both common strategies for the generation CDs in some early studies. These strategies involve a similar reorganiza-tion process of the carbon atoms decomposed from bulk carbon precursors by gas plasma generated in a sealed reactor [119]. However, the former is driven by ultra-high applied voltage, whereas the latter generates gas plasma via the use of a high-energy laser pulse. Generally speaking, CDs driven by these strategies exhibit poor fluorescence, thereby need to be further passivated by a polymer [9]. However, there are also a few reports about the one-step generation of surface-passivated CDs via laser ablation of a suspension of carbon powders in different organic solvents [43]. It has been demonstrated that the reaction condi-tions determine the performance of CDs (e.g., emission time and wavelength ablation source) [55]. Considering the harsh experimental condition required, currently there are few reports using these methods to generate CDs in the wake of develop-ments in CD-based materials chemistry.

Oxidative cleavage – that is oxidation cutting – is a more widely utilized strategy in comparison. This strategy refers to breaking the bulk carbon target (e.g., carbon fiber [105], CX-72 carbon black [29], candle soot [120], Super P [112]) into small-sized carbon dots through destroying carbon–carbon bonds in the presence of a strong oxidant. According to the different oxi-dation conditions, the oxidative cleavage process can be divided into two distinct categories: chemical oxidation and electrochemical oxidation process. In the chemical oxidation process, several assisted methods, including reflux and hydrothermal/-solvothermal treatments, are used to accelerate the reaction pro-gress [109]. The oxidant – typically a mixture of HNO_3/H_2SO_4 – can serve as a “scissors” to cut the carbon–carbon bonds of the bulk carbon target, resulting in the emergence of edge sites (Fig. 6b) [105,109] What's more, the reaction temperature and concentration of the oxidant can significantly influence the for-mation process of CDs, which can be used to regulate the size of CDs [121]. In the electrochemical oxidation strategy, the bulk carbon target is used as working electrode and then oxidatively cleaved into CDs at high redox potentials (Fig. 6c) [122,123]. The applied voltage is high enough to oxidize water, thereby resulting in the generation of hydroxyl and oxygen radicals, which act as electrochemical ‘‘scissors’’ to form CDs [124]. Dur-ing this process, the nature of CDs is usually regulated by the applied voltage and the pH of the solution. The value of the applied voltage is inversely proportional to the size of the CDs [42], and CDs generated in alkaline solution are apt to exhibit high crystallinity and benign optical properties [61,125].

A microfluidization strategy, which is usually used in fabrica-tion of oil-in-water nanoemulsions [126] was also introduced recently for the generation of CDs [127]. The term “microfluidization” involves a dynamic high-pressure homoge-nization process, which generates liquid velocities of 400 m/s and applies high shear rates ($>10^7$ s ^{1}) on solid particles. There-fore, GQDs with a hexagonal symmetry in the real and reciprocal spaces can be obtained from cutting fragmented graphene.

Bottom-up strategies

The bottom-up strategies of CDs preparation generally involve combustion/thermal strategies and template strategies [7]. Com-bustion/thermal strategies refer to the reorganization and car-bonization of the carbon atoms of a precursor driven by external heating. In principle, all carbon-containing precursors can be used to generate CDs via a combustion/thermal process, including citric acid [113], phenylenediamine [18,52,95], acetaldehyde [128], phloroglucinol [23], melamine [103], and natural biomass [129,130]. Depending to the origin of the exter-nal heat, the synthesis methods can be divided into distinct cat-egories: direct pyrolysis [53], microwave [82,131], ultrasonic treatment [115,132], hydrothermal/solvothermal treatment [18,54,133], plasma jet [129], and magnetic hyperthermia [12]. Direct pyrolysis involves the generation of CDs in a solvent-free solution, in which the carbonization process is incomplete and thus numerous by-products emerge. In comparison, micro-wave generation is a more fascinating and facile strategy to gen-erate CDs than direct pyrolysis because it can induce temperatures over 1000 LC within one minute [134]. The ultra-fast heating rates can be ascribed to the interaction of matter with electromagnetic radiation, and thus are independent of the thermal conductivity of the carbon materials [135].

During the hydrothermal/solvothermal process, CDs synthe-sis in the reaction solution is driven by high temperature and high vapor pressures. Accordingly, the nature of solvents – e.g., boiling point [54], polarity [26] – is a key factor in the generation of CDs. Most CDs generated in aqueous solutions exhibited near-ultraviolet emission by virtue of the high polarity of water, and

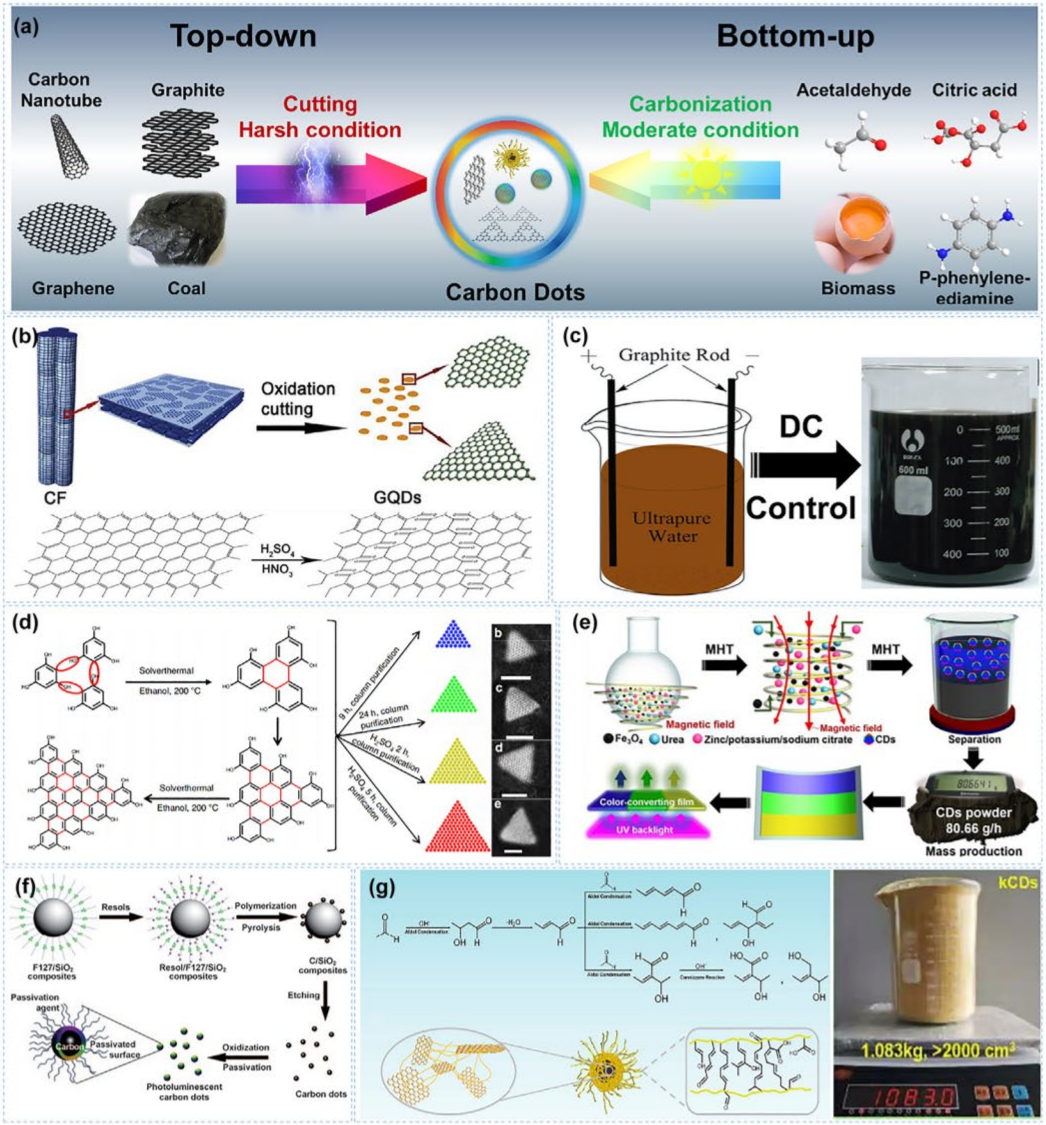

FIGURE 6

The fabrication of CDs. (a) Schematic depicting the fabrication strategies of CDs, including top-down and bottom-up strategies. (b) Schematic depicting chemical oxidation cutting of carbon fibers into CDs. Reproduced with permission [105]. Copyright 2012 American Chemical Society. (c) Schematic depicting the electrochemical synthesis of CDs. Reproduced with permission [123]. Copyright 2012 Royal Society of Chemistry. (d) Schematic depicting synthesis of triangular CQDs via a solvothermal strategy. Reproduced with permission [23]. Copyright 2018 Nature Publishing Group. (e) Schematic depicting synthesis of CDs via a magnetic hyperthermia strategy. Reproduced with permission [12]. Copyright 2020 Wiley-VCH. (f) Schematic depicting synthesis of CDs via a template strategy. Reproduced with permission [143]. Copyright 2009 Wiley-VCH. (g) Schematic depicting the synthesis of CDs based on the aldol condensation reaction (left) and a digital photo of CDs (right). Reproduced with permission [116]. Copyright 2021 American Chemical Society.

thus exhibited poor dispersibility in organic solvents with conju-gated structures [26]. Therefore, reaction solvents with low polar-ity are apt to induce the generation of CDs with long-wavelength emission. Additionally, the reaction time and the type of catalyst significantly influences the nature of CDs [136]. For instance, tri-angular CDs with full width at half maximum exceeding 80 nm was successfully prepared by relegating the reaction time and concentration of the catalyst (H_2SO_4) using solvothermal treat-ment (Fig. 6d) [23]. Hydrothermal reaction under vacuum condi-tions has been reported as well, highlighting the uniform size of CDs [137]. The use of a plasma jet is another strategy to create an active chemical environment containing abundant intrinsically charged particles, as well as excited neutral species for the rapid generation of CDs [138]. Although there are still few reports about this strategy, it is promising to be applied on a large-scale due to the advantage of a size-controllable and rapid-preparation [139–141].

Very recently, magnetic hyperthermia was reported as a method aiming at large-scale production of CDs [12]. During this process, an alternating electromagnetic field was applied into magnetic nanoparticles-incorporated systems, resulting in the emergence of a large amount of heat that will induce a burst of chemical reactions (Fig. 6e) [138]. This strategy enabled a large-scale and rapid production of CDs with a production efficiency of ca. 85 g/h and a yield of ca. 60%. Ultrasonic treatment was proposed to generate CDs in a one-step process as well

TABLE 1

Different synthesis strategies of CDs.

Classification	Preparation strategy	Preparation conditions	Advantages	Disadvantages	Refs.
Top-down	Arc discharge	Ar atmosphere, arc discharge	high-purity CQDs, high-efficiency	Wide size distribution of CDs, high energy-usage, expensive equipment	[8]
	Laser ablation	Ar atmosphere, laser	high-purity CQDs, high-efficiency	Wide size distribution of CDs, high energy-usage, expensive equipment	[9,55]
	Chemical oxidation	Strong oxidant, reflux/ hydrothermal/solvothermal	Well hydrophilicity and crystallinity of CDs	Low yield, time-consuming	[29,105]
	Electrochemical oxidation	Applied voltage	High-purity, high-efficiency, high-yield, and narrow size distribution of CDs	High energy-usage	[42,123]
	Microfluidization	Microfluidization	High yield	Expensive equipment	[127]
Bottom-up	Direct pyrolysis	Heating treatment	Easy operation, high-efficiency, solvent-free, wide precursor source	Wide size distribution of CDs, low QY of CDs	[53]
	Microwave	Microwave heating treatment	Easy operation, high-efficiency, high-yield, solvent-free, wide precursor source	Wide size distribution of CDs	[82,131]
	Ultrasonic	Ultrasonic treatment, acidic/alkaline solution	Wide size distribution of CDs, a high-efficient assisted-synthetic method	Low yield, time-consuming	[115,132]
	Hydrothermal/solvothermal strategy	High pressure, heating	Easy operation, easy-functionalized, high QY of CDs, wide precursor source	Low yield, time-consuming	[95,109]
	Aldol condensation	Strong acidic/alkaline solution	Room temperature, low energy consumption, low-cost, high yield	Low QY of CDs	[11,49]
	Template	Heating with template molecule	CDs with uniform size and specific nanostructure	Few available templates	[143,146]
	Plasma jet	Plasma treatment	High yield	High energy-usage, expensive equipment	[140,143]
	Magnetic hyperthermia	Magnetic hyperthermia treatment	High yield	Expensive equipment	[12]

[115,132]. During this process, carbon–carbon bonds in the pre-cursor are destroyed via instantaneous ultra-high energy induced by an ultrasonic wave [142].

The template strategy is an approach to generate CDs with specific morphology aided by a template molecule. Liu et al. [143] innovatively succeeded in synthesizing CDs via this strat-egy using SiO_2 spheres as the carriers and resols as the precursors (Fig. 6f). Using this foundation, a soft–hard template strategy was proposed to obtain CDs, which not only offered confined nanos-paces for the formation of CDs with specific morphology, but also avoided the aggregation of CDs during the high-temperature carbonization process [143]. Subsequently, several templates were proposed based on a similar mechanism, which generally used copolymers as a soft template or silica as a hard template [144,145]. Very recently, Tsukruk et al. [146] proposed the template-assisted assembly of CDs with large crystals (<200 lm) at the liquid–air interface. The various ligand-templated assemblies enabled the emergence of CDs with differ-ent crystal architectures (e.g., fibers, microplates and micro-flowers).

As is well known, the applications of CDs have been limited tremendously by their poor yield through traditional synthesis strategies for a long time. The question of “how to achieve large-scale fabrication of CDs” is urgent and needs to be solved. Accordingly, our group [11,49] first proposed a facile preparation strategy of CDs on a large-scale based on the aldol condensation reaction, which was carried out at room temperature and ambi-ent pressure in open system. Aldehydes or ketones with a-hydrogen (a-H) atoms can be converted to unsaturated aldehy-des or ketones under alkaline conditions, and then unsaturated aldehydes or ketones will undergo various substitution and con-densation reactions during the synthesis process. On the one hand, a vinylogy reaction occurs due to the conjugation effect of the double bond and the aldol reaction, resulting in the elon-gation of carbon chains. On the other hand, uncontrollable side reactions, such as the Cannizzaro reaction, can take place driven by a self-exothermic reaction, and results in the generation of carboxyl and hydroxyl group. Polymer chains with different functional groups and small clusters emerged and further curled, cross-linked and dehydrated to generate the carbon core of CDs. One has to keep in mind that functionalization of CDs is possible via incorporating various dopants. Very recently, we [116] updated the aforementioned preparation method of CDs and successfully achieved kilogram-scale synthesis of CDs (Fig. 6g).

Design of CDs-based nanohybrids

Loading strategies

The “a whole greater than the sum of the parts” effect can be achieved via the combination of CDs with various functional matrix materials. The fascinating surface states and ultra-high specific surface areas of CDs are necessary for the construction of CD-based nanohybrids. Hitherto, the loading strategies of CDs mainly consist of three types, that is, physical mixing, elec-trophoretic deposition (EPD), and heating treatments. The phys-ical mixing process is a facile and easy-to-operate strategy to achieve CD-based nanohybrids, in which CDs combine with var-ious materials (e.g. ZnO nanowire arrays [147], carbon nitride sheet [21], RuO_2 [148], tremella-like $NiCo_2O_4$ [149] and rubber [150]) through hydrogen-bonding, electrostatic interactions and p–p stacking interactions after a simple stirring or soaking treatment. For instance, a multilayer CD-based nanohybrid was obtained via a novel layer-by-layer assembly approach, in which metal particles with negative charges and CDs with positive charges were connected by electrostatic interactions (Fig. 7a) [151]. However, one has to keep in mind that these weak interac-tions are insufficient to offer long-term connections between CDs and the other materials in the matrix, thereby resulting in the failure of the nanohybrids eventually. Given this issue, the introduction of polymer binders (e.g. polyvinyl alcohol (PVA) [152], polyvinylidene fluoride (PVDF) [153]) are used to stabilize CD-based nanohybrids.

The EPD strategy consists of both electrophoresis and deposi-tion [154]. During EPD, CDs with negative or positive charges firstly transfer toward the working electrode (target material) with opposite charges driven by the applied electric field. CDs then start to accumulate around the surface of the working elec-trode, and finally CDs uniformly deposit on the surface of the target material (Fig. 7b). The deposition rate of CDs follows Hamaker's law (1):

dm=dt ¼ f lESC

where m refers to the deposition mass (g), and t refers to the deposi-tion time (s). f is a factor that takes into account that only a fraction of the particles transported to the electrode by electrophoresis is incor-porated in the deposit (f 1). l and E refer to electrophoretic mobility (m^2/V s) as well as the strength of electric field, respectively. S is the surface area of the electrode (m^2), and C is the concentration of the colloidal suspension (g/m^3). Therefore, the thickness of the deposition layer can be controlled by regulating the reaction time, the elec-trophoretic solution, and the electric field. Given that, various CD-based nanohybrids have been synthesized by EPD and some satisfac-tory results were obtained, in which CDs exhibited distinct loading morphologies (e.g., mossy [155], pine branches [156], and film [157]) via controlling the parameters. For instance, Yang et al. [158] reported that CDs can be anchored homogeneously onto $Na_2Ti_3O_7$ nanofiber arrays via EPD, as shown in Fig. 7c. It should be noted that an excessive thick deposition layer results in aggregation of CDs and blocks the nanostructure of the CD-based nanohybrids [159].

The heating treatment is the most frequently used strategy to produce nanohybrids, in which the chemical bonding (e.g., covalent binding) is achieved by external heating. In term of CD-based materials chemistry, the heating treatment can be divided to "dry" and "wet" processes according to the different heating atmospheres. The former means CD-nanohybrids are obtained under a solvent-free system, and typically an inert atmosphere (e.g., Ar) is needful to reduce the emergence of side reactions [160]. The latter refers to the formation of CD-based nanohybrids via hydrothermal/solvothermal treatments, which can offer a more homogeneous reaction solution in comparison [161]. For instance, Yuan et al. [162] prepared CD-coated reduced graphene oxide (rGO) composites through a hydrothermal pro-cess, in which a strong covalent bond was formed between CDs and rGO and thus CDs could be anchored homogeneously and tightly on the rGO matrix (Fig. 7d). The growth rate of CD-based nanohybrids is highly dependent on the heating time and temperature. More specially, single crystal nanostructures and larger sized CD-based nanohybrids emerge at relatively higher temperatures [163], whereas exorbitant temperatures will accelerate the decomposition CDs that leads the failure of CD-based nanohybrids [164].

Effect of CDs

The beneficial role of CDs in CD-based nanohybrids include the addition of: (1) designer additives, (2) stabilizing agents, (3) pho-tosensitizers, and (4) conducting mediators. As for designer addi-tives, our group [165] has demonstrated the influence of CDs on the morphology of CD-based nanohybrids (graphene-like carbon-TiO_2 composite). During the synthesis process, the pres-ence of CDs inhibits the random crystal growth of the matrix (e.g., rutile TiO_2). Instead, CDs induce the emergence of tiny nas-cent crystal nuclei that grow into the 1D linear nanoneedles. The linear nanoneedles coalesced with each other and then self-assembles to create the 3D structure (e.g., petal-like) thanks to the decrease of their surface energy. Additionally, it should be noted that the concentration of CDs plays a critical role in the morphology diversity of CD-based nanohybrids. For instance, Xiong et al. [166] synthesized CDs/$NiCo_2O_4$ nanohybrids with various morphologies through the hydrothermal method, such as urchin chestnut, flower, and bayberry, by adding 0, 0.25, 0.5, and 1.0 mg mL ^{1} of CDs, respectively (Fig. 7e). Likewise, a series of hybrid nanomaterials with distinct morphologies, including CDs/Mn_2O_3 [167], CDs/Bi_2WO_6 [168], and CDs/poly-mer [169] were later proposed.

The role of stabilizing agents means that CDs are able to main-tain the stability of the CD-based nanohybrid systems (e.g., col-loid). For instance, adding CDs can prevent metal nanoparticles (MNPs) (silver (Ag) [170,171], gold (Au) [171], palladium (Pd) [172]) from oxidation, as well as prevent aggregation in the aque-ous solution because of their high stability and hydrophilicity. In the presence of surface functional groups, especially hydroxyl groups (–OH), CDs are able to interact with MNPs via hydrogen bonding, and then the MNPs adsorb onto the CDs surface, thereby hindering their aggregation [171]. Moreover, CDs with a large zeta potential (e.g., ~71.2 mV) can also enhance the stabil-ity of CD/MNP colloids [172]. Likewise, CDs enable avoidance of the aggregation of other nanomaterials (e.g., reduced graphene oxide (rGO) [173], VO_2 interwoven nanowires [174]) as well. The benefit of CDs for stabilizing CD-based nanohybrids is also reflected by their chemical inertness, which can prevent the matrix from eroding in the reaction solution by coating on sur-faces of matrix [155]. In terms of the volume variation of CD-based nanohybrids, CDs also can serve as "toughening additives" to buffer the volume variation and thus boost the stability of the matrix [175].

The "photosensitizer" effect is another important role of CDs – much like traditional organic dyes – in optoelectronic devices [176]. Generally, sunlight cannot be used in its entirety (e.g., less

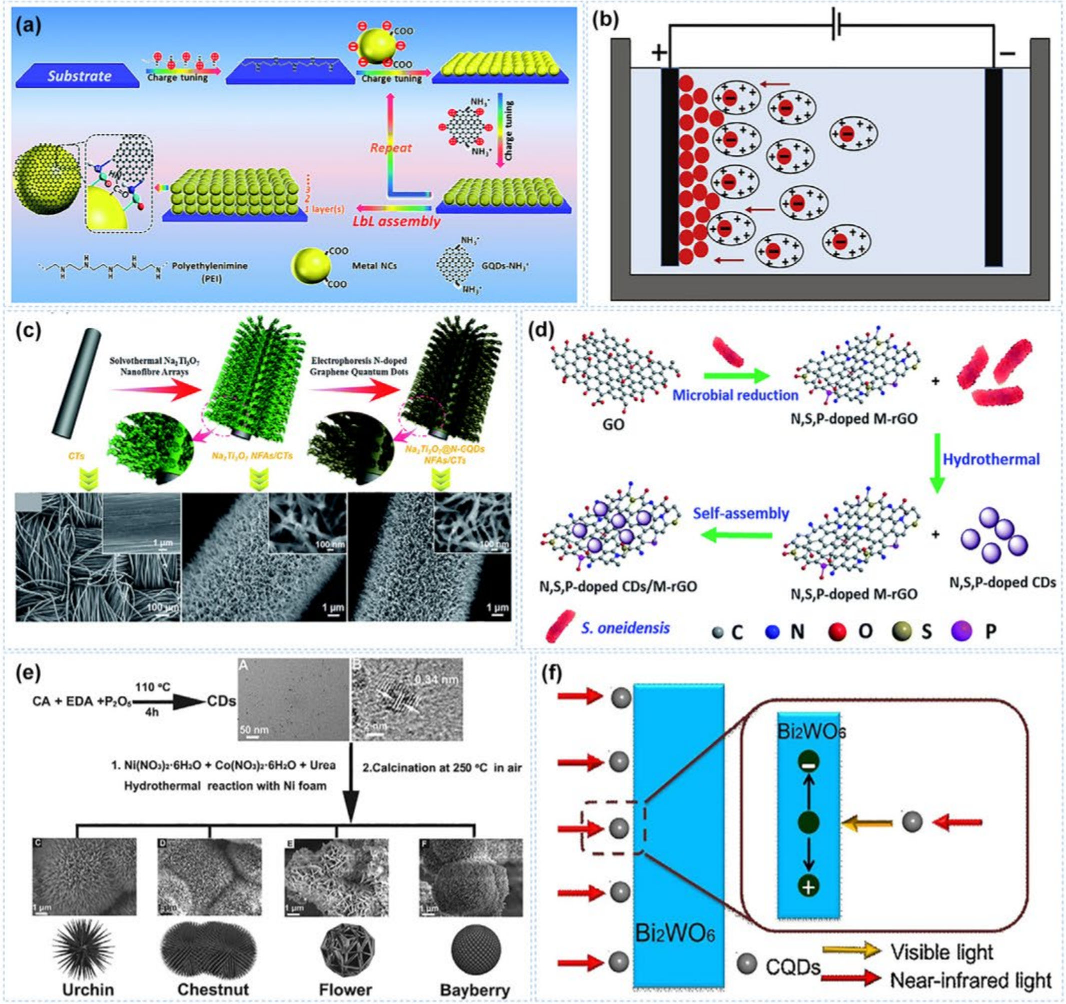

FIGURE 7

The fabrication and design of CD-based nanohybrids. (a) Schematic depicting the layer-by-layer assembly of metal particle/CD nanohybrids. Reproduced with permission [151]. Copyright 2018 Royal Society of Chemistry. (b) Schematic depicting the EPD process. Reproduced with permission [154]. Copyright 2018 Elsevier Ltd. (c) Schematic depicting the fabrication processes of CDs/$Na_2Ti_3O_7$/ carbon textiles nanohybrid via EPD strategies (top panel) and corresponding SEM images (bottom panel). Reproduced with permission [158]. Copyright 2019 Royal Society of Chemistry. (d) Schematic depicting the fabrication processes of CD/rGO nanohybrids via hydrothermal treatment. Reproduced with permission [162]. Copyright 2016 Royal Society of Chemistry. (e) Schematic depicting the fabrication processes of CDs and their beneficial role as designer additives. Reproduced with permission [166]. Copyright 2016 Wiley-VCH. (f) Schematic depicting the beneficial role of CDs for boosting charge separation of CD/Bi_2WO_6 nanohybrids. Reproduced with permission [178]. Copyright 2018 Elsevier Ltd.

than 5%) by traditional optoelectronic devices due to its large intrinsic band gap [61]. However, CDs with upconverted PL properties render strong luminescence in the UV range after exciting using visible light. Thus, CD-based nanohybrids usually possess longer wavelength light absorption than a bare matrix, thereby causing significant differences in their optoelectronic activity [177].

Among various CD-based nanohybrids, CDs are usually used as a "conducting mediator" to boost the charge/ion transfer by virtue of their ultra-high surface energy and electrochemical properties (in the Section "Properties of CDs"). On the one hand, numerous studies suggest that CDs can offer fast charge/ion conducting path-ways, and thus reduce the charge transfer resistance on the elec-trode/electrolyte interface [178]. For instance, Fan et al. [161] reported that the charge transfer resistance (R_{ct}) of VO_2 nanobelt arrays electrodes decreases from 190 to 120 X via coating CDs on their surface. Very recently, Wang et al. [179] suggested that the existence of CDs on the surface of Co_3O_4@CuO electrodes was ben-eficial for storing electrolytes, and thus led to a short pathway for the diffusion of Li^+ ions, resulting in a higher diffusion rate of Li^+ ions (1.36 10 ^{12}–8.86 10 ^{15} cm^2 s ^{1}) than the bare Co_3O_4@-CuO electrodes (8.21 10 ^{14}–7.82 10 ^{17} cm^2 s ^{1}). On the other hand, CDs can form a Z-scheme heterojunction with the semicon-ductor nanohybrids because of their tunable band gap [20,180], thereby boosting the electron/hole pair (e /h$^+$ pair) separation effi-ciency. For example, Tang et al. [178] suggested that the band gap hybridization between CDs and Bi_2WO_6 can boost the sunlight absorption of CDs/Bi_2WO_6 nanohybrids in the range of 450–800 nm (Fig. 7f), and thus improved the separation efficiency of the e /h$^+$ pair.

Application of CDs

Sensor applications

Combining the merits of quantum dots and carbon-based nano-materials, CDs have been widely applied in multiple different fields. Statistically, the usage of CDs in the sensor field is the most frequently reported in carbon dot-based applications (Fig. 1c). Generally, CD-based sensors give rise to a low limit of detection (LOD) and ultra-high selectivity. According to the var-ious mechanisms, CD-based sensors can be divided mainly into photoluminescence, electroluminescence and electrochemical sensors [79,181]. Luminescence sensors are mainly based on the quenching or preventing the quenching of CDs fluorescence emission in the presence of the analyte. Since Jin et al. [182] first presented a GQDs-based PL sensor to detect Fe^{3+} ions in 2012, the “analyte” has been expanded to metal ions [183], hydrogen ions [184], anions [185], organic molecules [186], inorganic molecules [187], biomacromolecules [188] and so on. For instance, Chi et al. [189] reported that polyamine-functionalized CDs exhibited high selectivity for the detection of Cu^{2+} ions with a LOD of 6 nM by virtue of the effective quenching effect of Cu^{2+} ions (Fig. 8a). Due to their ideal electro-chemical nature, CDs can serve as signal-amplifier in electrolumi-nescence and electrochemical sensing process as well [190]. Various characterization techniques have been employed for generating an electrochemical response, including voltammetry (CV), voltammetry differential pulse (DPV), square wave voltam-metry (SWV) or pulsed amperometry (PA) [90]. During this pro-cess, CDs will change the electroactivity of a target analyte (e.g. single-stranded DNA [191], troponin [192]) through covalently attaching to the analyte or by electrostatic repulsion, thereby resulting in a drastic decrease of the electrochemical signal. Addi-tionally, very recently, an emerging class of thermal-sensors were achieved based on exploiting the physicochemical properties of CDs by varying the temperature, which has been applied in the field of nanothermometers [193,194] and thermoelectric devices [195].

Bio-medical applications

Bio-medical science, which is widely praised as “the science of the 21st century”, is an obvious area for the application of CD-based materials chemistry. Compared to traditional organic fluo-rophores and semiconductor quantum dots, CDs are able to be used in vivo/vitro by virtue of their photobleaching, highly selec-tivity, biocompatibility and low cytotoxicity [19]. The applica-tion of CDs in this field can be divided into: bio-sensor, bio-imaging, drug/gene delivery and specific drug. To avoid repeti-tion, the application of CDs in sensor field is not described again. Firstly, the excellent PL nature of CDs means they have a large application potential in bio-imaging. In some early studies, CDs with near-ultraviolet emission were proposed as imaging agents, which might lead to irreversible radiation damage and overlap the background fluorescence in organisms [19]. There-fore, CDs with NIR emission/excitation became widely investi-gated in bio-imaging applications [136,196]. Xiong et al. [18] succeeded in using NIR emission (700 nm) CDs under visible light excitation (510 nm) for fluorescent imaging in living mice (Fig. 8b). Moreover, the high selectivity of CDs is an underlying factor for bio-imaging, which can aid diagnosis through deliver-ing information on the type and position of the targets [197]. To achieve selective targeting, a series of recognition moieties (e.g., folic acid [198], molecularly imprinted polymers [199], mono-clonal antibody [200]) were introduced in CDs that are able to connect with unique receptors on the target cell. For example, recently, Fan et al. [201] successfully utilized bio-imaging based on CDs to detect the early warning signs of tumorigenesis. The photoluminescence intensity of CDs can be boosted by nicoti-namide adenine dinucleotide, whose concentration is markedly higher in tumor cells than that of normal cells.

CDs and their nanohybrids are promising delivery systems for drug/gene molecules, because they exhibit outstanding carrying capacity induced by their chemical stability and ultra-high speci-fic surface area [202]. During drug/gene delivery, the drug/gene molecule will bind with the active sites on CDs via various load-ing mechanisms (p-p stacking [203], electrostatic [17], Schiff base linkage [204], noncovalent [16], and amide bond [205]). Hitherto, various drugs (e.g., paclitaxel [206], cisplatin (IV) [207], nitric oxide [208]) and gene molecules (e.g., small interfer-ing RNA [209], TNF-related apoptosis-inducing ligand [210]) have been successfully located on CDs during delivery process. Once contact with target sites occurs, drugs can be released by endogenous (e.g., the value of pH, as well as enzyme concentra-tion) and exogenous stimuli (e.g., applied light source, magnetic field, as well as ultrasound) (Fig. 8c) [19,211].

In addition, CDs and their nanohybrids also can be used directly as drugs against various disease, including bacterial ker-atitis [212], coronaviruses [213], Alzheimers [214], and Parkin-son’s disease [215]. On one hand, CDs and their nanohybrids exhibit well antibacterial activity via enhancing reactive oxygen species-induced oxidative stress of bacterial [216] and specific interaction with bacterial membranes [212,217], resulting in the rupturing of bacterial membranes and eventually bacterial death. On the other hand, various drug molecule (e.g., triazole [213]) can be grafted on the surface of CDs, imparting the med-ical application potential of CDs against human disease.

Energy applications

Numerous studies suggest that CDs can significantly increase the energy conversion and storage efficiency of various energy stor-age devices, including light-emitting diodes (LEDs) [22,98], solar cells (SCs) [218], rechargeable ion/metal batteries [11,15,49], supercapacitors [148,156,166] and so on [145]. In the LED field – especially white-emission LED (WLEDs) – CDs are an ideal alternative to the traditional phosphors, which consist of rare earth metals with non-negligible toxicity [218]. During the pack-aging process of LEDs, solid-state fluorescent CDs or CD-based nanohybrids (e.g., CD/starch [96], CD/polymethyl methacrylate hybrid) have been used to avoid the aggregation induced quenching effect. Additionally, WLEDs with various correlated color temperatures (CEE) can be achieved by regulating the ratio of red-, green- and blue-emission CDs [54]. Nevertheless, one has to keep in mind that the low fluorescent intensity of existing red-emission CDs results in the cool chromatic temperature of LEDs. Thus, CDs with white emission have been used directly in WLED fabrication recently (Fig. 8d) [52], which was more convenient by comparison. Besides, CDs can also play various beneficial roles

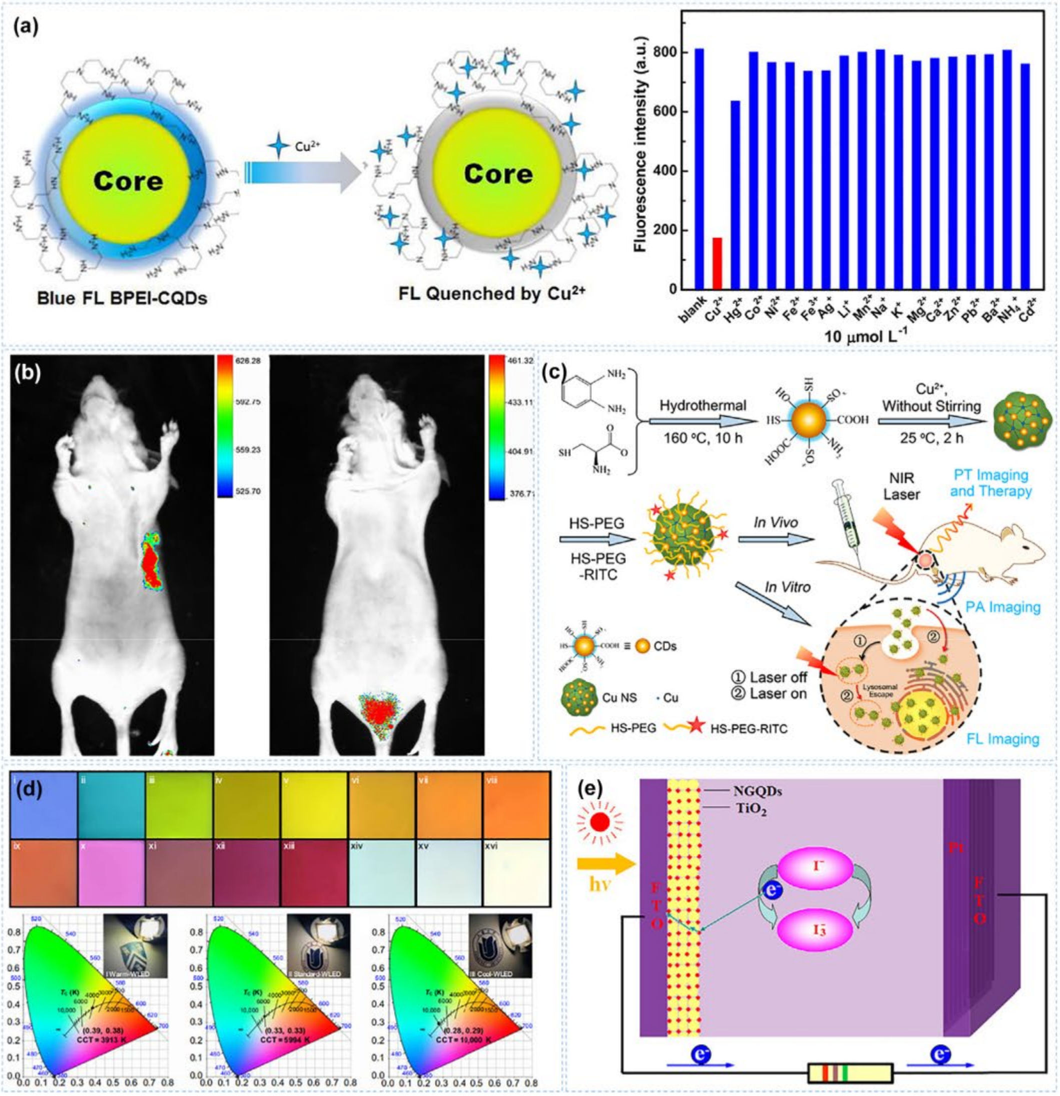

FIGURE 8

The recent advance of CDs in various fields (Ⅰ). (a) Schematic depicting the quenching effect of Cu^{2+} ions for polyamine-functionalized CDs (left) and normalized fluorescence intensity at polyamine-functionalized CDs solution in the presence of various metal ions (right) Reproduced with permission [189]. Copyright 2012 American Chemical Society. (b) Fluorescence images in-vivo of nude mice after subcutaneous injection (left) and intravenous injection (right) of red-CD solutions. Reproduced with permission [18]. Copyright 2016 American Chemical Society. (c) Schematic depicting the application of CDs in multimodal imaging-guided cancer treatment. Reproduced with permission [211]. Copyright 2018 American Chemical Society. (d) A digital photo of the applications of CDs in full-color fluorescent film (top panel) and WLED (bottom panel). Reproduced with permission [52]. Copyright 2020 American Association for the Advancement of Science. (e) Schematic depicting the device structure of CDs-sensitized TiO_2 solar cell. Reproduced with permission [220]. Copyright 2013 Elsevier Ltd.

(e.g., photosensitizers charge transporting medium, and active layer additives) in different types of solar cell, including semicon-ductor solar cells [219], perovskite solar cells [22], and dye-sensitized solar cells [220,221]. For instance, Huang et al. [220] introduced CDs as metal-free photosensitizers in solar cells (Fig. 8e), resulting in a power conversion efficiency of 0.13% in a proof-of-concept study under one sun illumination (AM 1.5).

The use of CDs in rechargeable ion/metal batteries and super-capacitors consists of three main types: directly using CDs, CD-based nanohybrids and CD-driven materials. There were some reports that CDs were directly used as electrode materials [222]. However, it might not be an ideal strategy due to its high-cost and unsatisfactory electrochemical performance. To achieve effi-cient utilization of CDs, CDs were recently employed as electrolyte additives (Fig. 9a) [100,223,224], which is praised as "vitamin" of electrolyte and their content was generally below 5% [225]. In comparison, CD-nanohybrids are the most popular way of utilizing CDs in this application, in which the beneficial effect of CDs is boosting of the ion/charge transfer (Fig. 9b) [161], designing [165] and stabilizing of the nanohybrids [175] and so on (as has been discussed in Section Effect of CDs). Additionally, a series of electrode materials with excellent electrochemical per-formance can be derived from CDs and their nanohybrids [226]. During thermal treatment, the carbon atom from the CDs will be reorganized and self-assemble into 1D carbon fibers (CF) [116], 2D large-size carbon nanosheets [49] or 3D porous carbon frameworks [11]. For instance, our group [128] utilized CD-based micelles to generate a hollow carbon anode for potassium ions

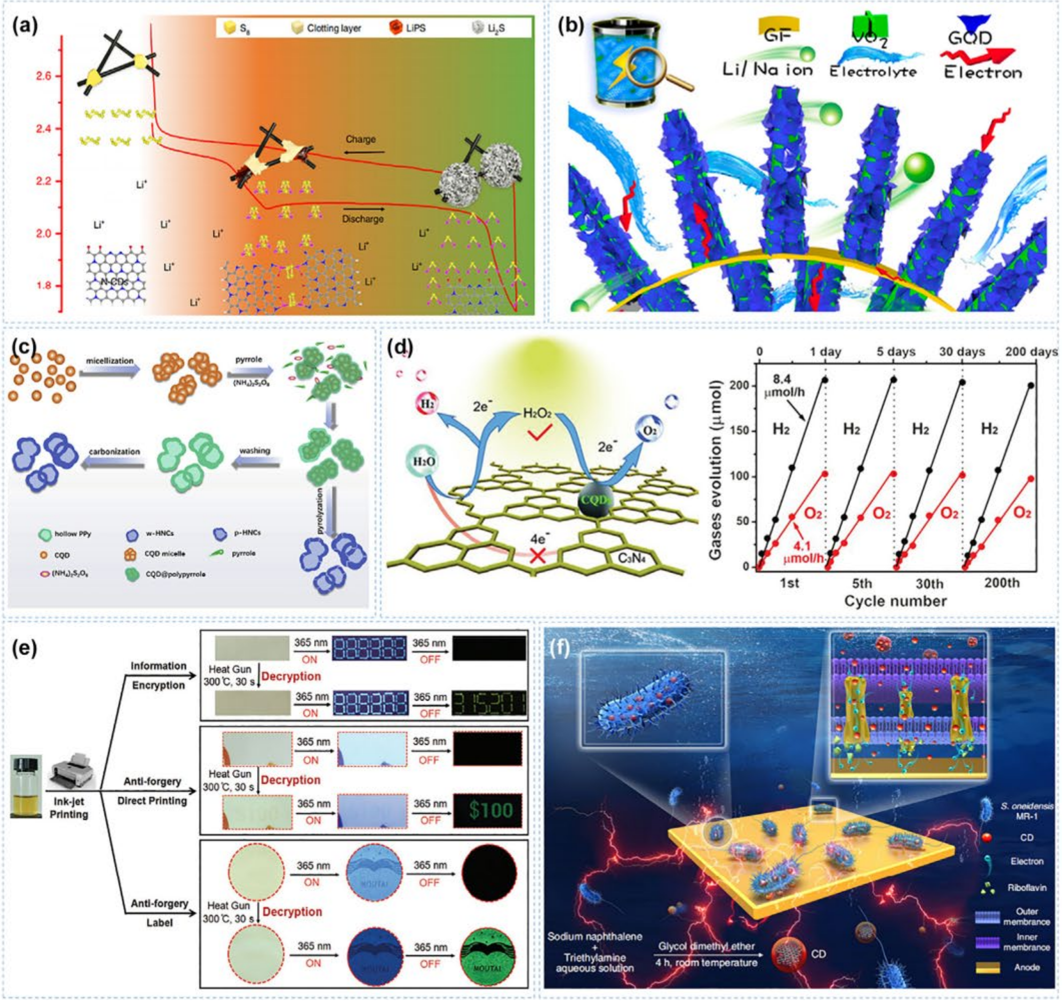

FIGURE 9

The recent advance of CDs in various fields (Ⅱ). (a) Schematic depicting the effect of CDs as electrolyte additives for blocking the shuttle effect of lithium polysulfides in lithium-sulfur batteries. Reproduced with permission [223]. Copyright 2020 Nature Publishing Group. (b) Schematic depicting the beneficial effect of CDs for charge transfer in lithium/sodium ion batteries. Reproduced with permission [161]. Copyright 2014 American Chemical Society. (c) Schematic depicting the synthesis process of hollow N-doped carbon driven by CDs. Reproduced with permission [128]. Copyright 2019 Elsevier Ltd. (d) Schematic depicting the effect of CDs/C_3N_4 nanohybrids for photocatalytic overall water splitting (left), and a typical time curve of H_2 and O_2 gas generation from water under visible light irradiation in the presence of CD/C_3N_4 nanohybrids (right). Reproduced with permission [232]. Copyright 2015 American Association for the Advancement of Science. (e) A digital photo of the CD-based ink and their use in anti-counterfeiting applications. Reproduced with permission [234]. Copyright 2018 Wiley-VCH. (f) Schematic depicting the effect of CDs-fed cells for enhanced bioelectricity generation. Reproduced with permission [238]. Copyright 2020 Nature Publishing Group.

batteries, in which CDs served multiple roles of a template and pore-forming agent, simultaneously (Fig. 9c).

Catalysis applications

The catalysis application of CDs mainly consists of photocataly-sis and electrocatalysis, which are driven by an applied light source and an applied electric field, respectively. It has been demonstrated that catalysis has a significant impact on various environmental protection and energy conversion issues, includ-ing CO_2 conversion [68,227], water splitting [30,147,228], organic pollutant degradation [159,168,178,229] and so on. CDs-based catalysts have been stimulating more wide research interest compared to the traditional catalysts in term of their low toxicity and cost. On the one hand, pure CDs can serve directly as catalysts owing to their quantum confinement effects. Li et al. [230] firstly proposed colloidal CDs as a promising cata-lyst for the oxygen reduction reaction (ORR), albeit with the fact that its electrocatalytic activitie was slightly inferior to that of Pt/ C electrode. What's more, it was also indicated that the better catalysis performance of pure CDs can be obtained via narrowing their gap band [230]. On the other hand, CDs can be involved as catalysts by combining with various materials (e.g., noble metal [231], metal oxide [39,61,78,176], grapheme [162], carbon nitride [21,232]) in a matrix, resulting in boosting the charge sep-aration, offering more reactive sites, as well as reducing the acti-vation energy for product evolution. For instance, Kang et al.

[232] innovatively proposed a metal-free CDs/g-C_3N_4 nanohy-brid to split water in two steps through visible light excitation. This nanohybrid exhibited ideal photocatalyst activity and solar energy conversion efficiency (~2.0%) and maintained an excel-lent performance even after 200 cycling tests over 200 days (Fig. 8d).

Other applications

With the increasing research interest towards carbon dot-based materials chemistry, CDs are now being investigated in more and more applications. For instance, owing to their unique solid-state fluorescent and phosphorescence nature, it comes as no surprise that CDs are a promising material in the field of secu-rity, including for fingerprint detection [233] and anti-counterfeiting signatures (Fig. 9e) [85,86,103,234]. Additionally, the beneficial effect of CDs in mineralogy [235], MRI contrasting agents [236], membrane separation [237], and bacteria feeding (Fig. 9f) [238] applications have been reported.

Conclusions and prospects

In general, carbon dots-based materials chemistry is an emerging subject in the nanomaterials field, which has been developing and enriching since 2006. Although enormous progress has been made, there are continuing debates on the following issues: (1) what is the exact nature of carbon dots? (2) what are the design principles of carbon dots and their nanohybrids? (3) what is the working mechanism of carbon dots and their derived materials in various applications? (4) how to prepare carbon dots with the desired features on a large scale but with low cost? Therefore, herein, we divided carbon dots into five types and discussed their physicochemical features (see Table 2). The design principle of carbon dots has been discussed, showing that the performance of carbon dots is highly dependent on their tunable band gap, which varies with their quantum size and surface state. Further-more, the design principle of carbon dots was discussed in terms of loading strategies and the beneficial role of carbon dots in applications. Finally, the recent advances of carbon dots and their nanohybrid were summarized.

Hitherto, although a great distance remains from commercial applications of carbon dots, we believe that it is absolutely feasi-ble given the rapid development of CDs-based materials chem-istry. We propose key directions for this promising field as:

(1) “Being better”, which means that the performance of car-bon dots needs to be further optimized. For instance, the photoluminescence properties of carbon dots remain infe-rior to commercial semiconductor quantum dots in terms of quantum yield. Especially, the fluorescence intensity of red-emission does not yet match with the existing demand, and limits their application in photoelectric devices. Additionally, carbon dots with poor chemical inertness also bring a risk of cyotoxicity when used in biomedical applications. Thus, we expect this point remains the main challenge in the development of carbon dots.

TABLE 2

The difference between various CDs.

Type	Structural characteristic	PL mechanism	Fabrication strategy	Advantages	Disadvantages	Suitable application	Ref
GQDs	A few layers graphene plane, thickness <2 nm and lateral dimensions <10 nm, graphitic domains framework, functional groups on the surface/edges	The quantum confinement effect and surface/edge state	Top-down strategy and bottom-up strategy	High crystallinity, efficient electron transfer, low toxicity	Low yield, expensive, low QY, poor liposolubility	Solar cell, rechargeable batteries, supercapacitor, electrochemical sensing, photo/electrocatalysis	[58,60,181]
CNQDs	A few layers carbon nitride plane, thickness <6 nm and lateral dimensions <10 nm, poly(tri-s-triazine) framework, functional groups (typically amine) on the on the surface/edges	The quantum confinement effect and surface/edge state	Top-down strategy	Fast charge transfer, good chemical inertness, low toxicity, up-conversion PL	Low yield, expensive, poor liposolubility	Photocatalysis, LED	[38,39]
CQDs	The quasi-spherical nanoparticles, diameter <10 nm, complete carbonization core with obvious crystal lattice, functional group on the surface	The quantum confinement effect, the surface state and molecule state	Top-down strategy andbottom-up strategy	Easy functionalization, high specific surface area, high QY, low toxicity	Low yield, poor charge transfer	Sensing, bioimaging, drug delivery, LED, photocatalysis	[10,28,79]
CNDs	The quasi-spherical nanoparticles, diameter <10 nm, an amorphous structural core without crystal lattice, functional group on the surface	The quantum confinement effect, the surface state and molecule state	Bottom-up strategy	Easy functionalization, cheap, wide precursor source, high yield, low toxicity	Poor charge transfer, low crystallinity	Sensing, bioimaging, drug delivery, LED, carbon-based precursor	[7,26,44]
CPDs	The quasi-spherical nanoparticles, diameter size <10 nm, polymer/carbon hybrid framework, functional group on the surface	The quantum confinement effect, surface state and the crosslink enhanced emission effect	Bottom-up strategy	High yield, good chemical inertness, high QY, phosphorescence, chirality	Poor charge transfer, high toxicity of polymer	Sensing, LED, anti-counterfeiting, carbon-based precursor	[26,27]

(2) "Being cheaper", that is the fabrication strategies of carbon dots including cost-effectiveness, meaning that industrial-scale production will be a hotspot in the future. Currently, more and more studies focus on the large-scale fabrication of carbon dots [137], and even kilogram-scale synthesis of carbon dots have been achieved [116]. We expect that these gratifying achievements are a great start to achieve lower cost carbon dots.

(3) "Being smarter", that is more intelligent and normalized synthesis routes will be established by means of various method (e.g., artificial intelligence technology [74]). To develop a normalized synthesis approach, simple organic molecules (e.g., citric acid, phenylenediamine, and acetaldehyde) are more likely to be used as synthetic units for the preparation of carbon dots than biomass materials.

(4) "Being more precise", which means that the studies focus-ing on the behavior of single CDs or clusters of a few car-bon dots are more likely to be reasonable. Just as throwing gold into sand, some specific features of carbon dots are generally apt to be neglected while considering the behavior of carbon dots macroscopically. For instance, Nguyen et al. [239] recently observed the energy flow within or between single carbon dots via ultrafast nano-metric imaging. Interestingly, their analysis suggested that there are nearly 20% of carbon dots with ultrahigh fluores-cent intensity, whereas others had poor fluorescent behav-ior or were without fluorescence. Therefore, it was suggested that the "near-prefect" carbon dots, whose fluo-rescent intensity was comparable with that of semiconduc-tor quantum dots, could be obtained merely through improved separation. Of course, various advanced charac-terization and separation techniques are required to resolve this issue as well.

Last but not least, we believe that progress of carbon dots - based materials development will significantly influence the evolution of materials science, just as that of graphene!

Declaration of Competing Interest

The authors declare that they have no known competing financial interests or personal relationships that could have appeared to influence the work reported in this paper.

Acknowledgements

This work was financially supported by the National Natural Science Foundation of China (52074539, 51904342), National Key Research and Development Program of China (2017YFB010200), Hunan Provincial Science and Technology Plan (2020JJ3048), the Science and Technology Innovation Pro-gram of Hunan Province (2020RC4005, 2019RS1004), Innova-tion Mover Program of Central South University (2020CX007), and the Nature science of Shanxi Province (201801D121281).

References

[1] P. Cai et al., Adv. Energy Mater. (2021) 2003804.
[2] C.J. Brabec et al., Adv. Mater. 22 (2010) 3839–3856.
[3] R.H. Baughman et al., Science 297 (2002) 787–792.
[4] S. Stankovich et al., Nature 442 (2006) 282–286.
[5] Z.-Y. Wang et al., Rare Metals 39 (2020) 1383–1394.
[6] G.-T. Song et al., Rare Metals 39 (2020) 784–791.
[7] S.N. Baker et al., Angew. Chem., Int. Ed. 49 (2010) 6726–6744.
[8] X.Y. Xu et al., J. Am. Chem. Soc. 126 (2004) 12736–12737.
[9] Y.-P. Sun et al., J. Am. Chem. Soc. 128 (2006) 7756–7757.
[10] K. Nekoueian et al., Chem. Soc. Rev. 48 (2019) 4281–4316.
[11] H. Hou et al., Adv. Mater. 27 (2015) 7861–7866.
[12] Z. Zhu et al., Angew. Chem., Int. Ed. 59 (2020) 3099–3105.
[13] A. Cayuela et al., Chem. Commun. 52 (2016) 1311–1326.
[14] B.K. Walther et al., Mater. Today 39 (2020) 23–46.
[15] R. Guo et al., Energy Storage Mater. 37 (2021) 8–39.
[16] Q. Wang et al., Carbon 59 (2013) 192–199.
[17] H. Ding et al., ACS Appl. Mater. Interfaces 7 (2015) 6889–6897.
[18] H. Ding et al., ACS Nano 10 (2016) 484–491.
[19] J. Du et al., Small 15 (2019) 1805087.
[20] M. Han et al., Nano Today 19 (2018) 201–218.
[21] J. Liu et al., Appl. Catal. B 207 (2017) 429–437.
[22] X. Zhang et al., Adv. Funct. Mater. 30 (2020) 1910530.
[23] F. Yuan et al., Nat. Commun. 9 (2018) 2249.
[24] A.B. Bourlinos et al., Small 4 (2008) 455–458.
[25] C. Hu et al., Chem. Soc. Rev. 48 (2019) 2315–2337.
[26] S. Zhu et al., Nano Res. 8 (2015) 355–381.
[27] C. Xia et al., Adv. Sci. 6 (2019) 1901316.
[28] X.T. Zheng et al., Small 11 (2015) 1620–1636.
[29] Y. Dong et al., J. Mater. Chem. 22 (2012) 8764–8766.
[30] T.-F. Yeh, et al., Adv. Mater., 26 (2014) 3297-+.
[31] X. Li et al., J. Mater. Chem. C 1 (2013) 7308–7313.
[32] K.A. Ritter et al., Nat. Mater. 8 (2009) 235–242.
[33] X. Wang et al., Chem. Soc. Rev. 45 (2016) 2239–2262.
[34] S.W. Yang et al., Adv. Mater. 29 (2017) 7.
[35] L. He et al., Mater. Today 22 (2019) 76–84.
[36] X. Wang et al., Nat. Mater. 8 (2009) 76–80.
[37] J. Zhou et al., Chem. Commun. 49 (2013) 8605–8607.
[38] Q. Cui et al., Angew. Chem., Int. Ed. 55 (2016) 3672–3676.
[39] G. Li et al., Nano Energy 19 (2016) 446–454.
[40] H. Nie et al., Chem. Mater. 26 (2014) 3104–3112.
[41] D. Li et al., Light Sci. Appl. 5 (2016) e16120.
[42] L. Bao et al., Adv. Mater. 23 (2011) 5801–5806.
[43] S.-L. Hu et al., J. Mater. Chem. 19 (2009) 484–488.
[44] J.T. Margraf et al., J. Phys. Chem. B 119 (2015) 7258–7265.
[45] A.B. Siddique et al., Mater. Chem. Phys. 249 (2020) 122984.
[46] A.B. Siddique et al., Sci. Rep. 8 (2018) 9770.
[47] S. Zhu et al., Chem. Commun. 50 (2014) 13845–13848.
[48] J. Shao et al., Adv. Sci. 4 (2017) 1700395.
[49] H. Hou et al., Adv. Sci. 4 (2017) 1600243.
[50] J. Ge et al., Adv. Mater. 27 (2015) 4169–4177.
[51] S.J. Zhu et al., Angew. Chem., Int. Ed. 54 (2015) 14626–14637.
[52] L. Wang et al., Sci. Adv. 6 (2020) eabb6772.
[53] M.J. Krysmann et al., J. Am. Chem. Soc. 134 (2012) 747–750.
[54] H. Ding et al., Small 14 (2018) 1800612.
[55] D. Reyes et al., Nanoscale Res. Lett. 11 (2016) 424.
[56] D.-W. Wang, D. Su, Energy Environ. Sci. 7 (2014) 576–591.
[57] L.B. Li et al., J. Mater. Chem. C 6 (2018) 7944–7970.
[58] Y. Yan et al., Adv. Mater. 31 (2019) 1808283.
[59] T.-F. Yeh et al., J. Phys. Chem. Lett. 7 (2016) 2087–2092.
[60] S. Zhu et al., Nano Today 13 (2017) 10–14.
[61] H. Li et al., Angew. Chem., Int. Ed. 49 (2010) 4430–4434.
[62] G. Eda et al., Adv. Mater. 22 (2010) 505–509.
[63] M.A. Sk et al., J. Mater. Chem. C 2 (2014) 6954–6960.
[64] L. Bao, et al., Adv. Mater., 27 (2015) 1663-+.
[65] X. Kou et al., Dalton. Trans. 49 (2020) 6915–6938.
[66] K. Hola et al., ACS Nano 11 (2017) 12402–12410.
[67] H. Tetsuka et al., Adv. Mater. 28 (2016) 4632–4638.
[68] Y. Yan et al., ACS Nano 12 (2018) 3523–3532.
[69] Y. Ru et al., Nano Today 34 (2020) 100953.
[70] F. Li et al., Angew. Chem., Int. Ed. 57 (2018) 2377–2382.
[71] F. Copur et al., Sens. Actuators B Chem. 279 (2019) 305–312.
[72] L.L. Zhou et al., ACS Appl. Nano Mater. 3 (2020) 946–952.
[73] M. Vazquez-Nakagawa et al., Chem. Commun. 52 (2016) 665–668.
[74] Y. Han et al., ACS Nano 14 (2020) 14761–14768.
[75] J. Zhou et al., J. Am. Chem. Soc. 129 (2007) 744–745.
[76] Y. Wang et al., J. Phys. Chem. Lett. 5 (2014) 1412–1420.
[77] B. Yao et al., Trends Chem. 1 (2019) 235–246.
[78] G. Muthusankar et al., Sens. Actuators B Chem. 281 (2019) 602–612.

[79] M. Li et al., ACS Sens. 4 (2019) 1732–1748.
[80] H. Ding et al., J. Appl. Phys. 127 (2020) 21.
[81] S.Y. Lim et al., Chem. Soc. Rev. 44 (2015) 362–381.
[82] K. Jiang et al., Angew. Chem., Int. Ed. 57 (2018) 6216–6220.
[83] L. Cao, et al., J. Am. Chem. Soc., 129 (2007) 11318-+.
[84] S. Zhu et al., Adv. Funct. Mater. 22 (2012) 4732–4740.
[85] K. Jiang et al., Angew. Chem., Int. Ed. 55 (2016) 7231–7235.
[86] S. Tao et al., Angew. Chem., Int. Ed. 57 (2018) 2393–2398.
[87] Q. Li et al., Nat. Commun. 9 (2018) 734.
[88] A. Ambrosi et al., Chem. Rev. 114 (2014) 7150–7188.
[89] D. Chen et al., Chem. Soc. Rev. 39 (2010) 3157–3180.
[90] D.B. Shinde et al., Angew. Chem., Int. Ed. 52 (2013) 2482–2485.
[91] R.B. Chen et al., Physica E Low Dimens. Syst. Nanostruct. 42 (2010) 2812– 2815.

[92] W. Wu et al., Angew. Chem., Int. Ed. 54 (2015) 6540–6544.
[93] C.E. Probst et al., Adv. Drug Deliv. Rev. 65 (2013) 703–718.
[94] C. Shen et al., J. Mater. Chem. C 3 (2015) 6668–6675.
[95] K. Jiang et al., Angew. Chem., Int. Ed. 54 (2015) 5360–5363.
[96] M. Sun et al., Nanoscale 6 (2014) 13076–13081.
[97] P.-C. Hsu et al., Chem. Commun. 48 (2012) 3984–3986.
[98] A. Panniello et al., J. Phys. Chem. C 122 (2018) 839–849.
[99] P. Zhao et al., Chem. Commun. 54 (2018) 5401–5406.
[100] D.K. Hong et al., J. Mater. Chem. A 7 (2019) 20325–20334.
[101] Q. Wang et al., J. Mater. Chem. C 8 (2020) 4343–4349.
[102] D. Pan et al., J. Mater. Chem. 21 (2011) 3565–3567.
[103] H. Yang et al., Nat. Commun. 10 (2019) 1789.
[104] H. Wang et al., Nanoscale 9 (2017) 1909–1915.
[105] J. Peng et al., Nano Lett. 12 (2012) 844–849.
[106] M. Nurunnabi et al., ACS Nano 7 (2013) 6858–6867.
[107] Z. Bagheri et al., Ecotoxicol. Environ. Saf. 161 (2018) 245–250.
[108] Y.-Y. Liu et al., Nat. Commun. 12 (2021) 812.
[109] D. Pan, et al., Adv. Mater., 22 (2010) 734-+.
[110] C.K. Chua et al., ACS Nano 9 (2015) 2548–2555.
[111] Y.T. Yew et al., Appl. Mater. Today 7 (2017) 138–143.
[112] Y. Zhu et al., Nanomicro. Lett. 12 (2020) 16.
[113] J. Schneider et al., J. Phys. Chem. C 121 (2017) 2014–2022.
[114] A.H. Loo et al., ACS Appl. Mater. Interfaces 8 (2016) 1951–1957.
[115] Z. Ma et al., New J. Chem. 36 (2012) 861–864.
[116] L. Li et al., ACS Nano (2021), https://doi.org/10.1021/acsnano.1020c10624.
[117] N. Tarasenka et al., Chemphyschem 18 (2017) 1074–1083.
[118] P. Russo et al., Nanoscale 6 (2014) 2381–2389.
[119] N. Arora et al., Diam. Relat. Mater. 50 (2014) 135–150.
[120] H.P. Liu et al., Angew. Chem., Int. Ed. 46 (2007) 6473–6475.
[121] D. Sun et al., Carbon 64 (2013) 424–434.
[122] Q.-L. Zhao et al., Chem. Commun. (2008) 5116–5118.
[123] H. Ming et al., Dalton. Trans. 41 (2012) 9526–9531.
[124] K. Li et al., J. Mater. Chem. B 5 (2017) 4811–4826.
[125] M. Liu et al., Analyst 141 (2016) 2657–2664.
[126] L. Bai et al., Food Hydrocoll. 61 (2016) 703–711.
[127] M. Buzaglo et al., Chem. Mater. 28 (2016) 21–24.
[128] W. Hong et al., Nano Energy 65 (2019) 104038.
[129] J. Wang et al., Angew. Chem., Int. Ed. 51 (2012) 9297–9301.
[130] H. Ding et al., J. Mater. Chem. B 5 (2017) 5272–5277.
[131] H. Zhu et al., Chem. Commun. (2009) 5118–5120.
[132] H. Li et al., Carbon 49 (2011) 605–609.
[133] F. Wang et al., Chem. Mater. 22 (2010) 4528–4530.
[134] K. MacKenzie et al., Sep. Purif. Technol. 66 (2009) 209–222.
[135] A.M. Schwenke et al., Adv. Mater. 27 (2015) 4113–4141.
[136] Z. Zhu et al., Mater. Today 30 (2019) 52–79.
[137] H. Zhao et al., Energy Environ. Sci. 14 (2021) 396–406.
[138] X.-Y. Du et al., Angew. Chem., Int. Ed. 60 (2020) 8585–8595.
[139] H. Jiang et al., Langmuir 26 (2010) 1991–1995.
[140] C.-X. Li et al., J. Mater. Sci. 48 (2013) 6307–6311.
[141] J. Kim et al., ACS Nano 8 (2014) 4190–4196.
[142] W. Chen et al., Nanotechnol. Rev. 7 (2018) 157–185.
[143] R. Liu et al., Angew. Chem., Int. Ed. 48 (2009) 4598–4601.
[144] J.M. Zhang et al., Chem. Eur. J. 21 (2015) 15142–15147.
[145] Y. Mu et al., Chem. Sci. 7 (2016) 3564–3568.
[146] R. Xiong et al., Angew. Chem., Int. Ed. 59 (2020) 20167–20173.
[147] C.X. Guo et al., Adv. Energy Mater. 3 (2013) 997–1003.
[148] Y. Zhu et al., Energy Environ. Sci. 6 (2013) 3665–3675.
[149] J. Luo et al., Carbon 146 (2019) 1–8.
[150] P. Yu et al., Compos. Commun. 22 (2020) 100429.
[151] Z. Zeng et al., J. Mater. Chem. A 6 (2018) 1700–1713.
[152] S. Wu et al., Adv. Opt. Mater. 6 (2018) 1701150.
[153] Y. Hu et al., Adv. Energy Mater. 9 (2019) 1802955.
[154] Y. Ma et al., J. Materiomics 4 (2018) 108–120.
[155] C. Zhu et al., Adv. Mater. Interfaces 2 (2015) 1400499.
[156] W.-W. Liu et al., Adv. Funct. Mater. 23 (2013) 4111–4122.
[157] Y. Hu et al., Nanotechnology 24 (2013) 195401.
[158] D. Kong et al., J. Mater. Chem. A 7 (2019) 12751–12762.
[159] Q. Wang et al., Nanoscale 9 (2017) 16046–16058.
[160] Y. Yang et al., J. Mater. Chem. A 3 (2015) 5648–5655.
[161] D. Chao et al., Nano Lett. 15 (2015) 565–573.
[162] L. Zhou et al., J. Mater. Chem. A 4 (2016) 7222–7229.
[163] B.B. Chen et al., Green Chem. 22 (2020) 4034–4054.
[164] T. Samanta et al., New J. Chem. 39 (2015) 106–109.
[165] Y. Zhang, et al., Adv. Mater., 28 (2016) 9391-+.
[166] J.-S. Wei et al., Small 12 (2016) 5927–5934.
[167] M. Jing et al., J. Mater. Chem. A 3 (2015) 16824–16830.
[168] J. Di et al., Appl. Catal. B 168 (2015) 51–61.
[169] A. Shakeel et al., ACS Nano 13 (2019) 9397–9407.
[170] S. Chen et al., Anal. Chem. 86 (2014) 6689–6694.
[171] Y. Su et al., ACS Sustain. Chem. Eng. 4 (2016) 1728–1735.
[172] P. Fageria et al., Langmuir 32 (2016) 10054–10064.
[173] X. Yun et al., ACS Appl. Mater. Interfaces 11 (2019) 36970–36984.
[174] M.-S. Balogun et al., ACS Appl. Mater. Interfaces 8 (2016) 9733–9744.
[175] J. Guo et al., J. Mater. Chem. A 4 (2016) 4783–4789.
[176] H. Yu et al., J. Mater. Chem. A 2 (2014) 3344–3351.
[177] Y. Lei et al., Appl. Catal. B 216 (2017) 59–69.
[178] J. Wang et al., Appl. Catal. B 222 (2018) 115–123.
[179] M. Wu et al., Chem. Eng. J. 373 (2019) 985–994.
[180] H. Li et al., Nanoscale 6 (2014) 867–873.
[181] H. Sun et al., Mater. Today 16 (2013) 433–442.
[182] D. Wang et al., Carbon 50 (2012) 2147–2154.
[183] Y. Guo et al., Biosens. Bioelectron. 63 (2015) 61–71.
[184] W. Shi et al., Angew. Chem., Int. Ed. 51 (2012) 6432–6435.
[185] H. Zhang et al., ACS Sens. 1 (2016) 875–881.
[186] J. Chen et al., Sens. Actuators B Chem. 252 (2017) 9–16.
[187] Z. Li et al., Sens. Actuators B Chem. 241 (2017) 821–827.
[188] Q. Huang et al., Biosens. Bioelectron. 94 (2017) 507–512.
[189] Y. Dong et al., Anal. Chem. 84 (2012) 6220–6224.
[190] J. Xi et al., ACS Appl. Mater. Interfaces 8 (2016) 22563–22573.
[191] J. Zhao et al., Electrochem. Commun. 13 (2011) 31–33.
[192] D. Bhatnagar et al., Int. J. Biol. Macromol. 95 (2017) 505–510.
[193] L.J. Mohammed et al., Nanoscale Res. Lett. 15 (2020) 182.
[194] Y. Xu et al., Anal. Chem. 92 (2020) 15632–15638.
[195] S. Li et al., ACS Appl. Mater. Interfaces 9 (2017) 3677–3685.
[196] H. Ding et al., J. Lumin. 211 (2019) 298–304.
[197] K.O. Boakye-Yiadom et al., Int. J. Pharm. 564 (2019) 308–317.
[198] J. Zhang et al., Talanta 183 (2018) 39–47.
[199] B. Demir et al., ACS Appl. Mater. Interfaces 10 (2018) 3305–3313.
[200] C. Han et al., J. Mater. Chem. B 4 (2016) 5798–5802.
[201] J. Li et al., Adv. Mater. 33 (2021) 2005096.
[202] N. Gong et al., Nat. Nanotechnol. 14 (2019) 379–387.
[203] T. Sun et al., Mater. Chem. Front. 1 (2017) 354–360.
[204] X. Jia et al., ACS Biomater. Sci. Eng. 2 (2016) 1641–1648.
[205] H.U. Lee et al., Sci. Rep. 4 (2014) 4665.
[206] H. Wang et al., Small 12 (2016) 6388–6397.
[207] T. Feng et al., ACS Appl. Mater. Interfaces 8 (2016) 18732–18740.
[208] J. Xu et al., Small 10 (2014) 3750–3760.
[209] S. Kim et al., Nano Res. 10 (2017) 503–519.
[210] H. Zhao et al., Chem. Mater. 30 (2018) 3438–3453.
[211] Y.-W. Bao et al., ACS Appl. Mater. Interfaces 10 (2018) 1544–1555.
[212] H.-J. Jian et al., ACS Nano 11 (2017) 6703–6716.
[213] P. Garg et al., Nano Today 35 (2020) 101001.
[214] Y.J. Chung et al., ACS Nano 14 (2020) 16973–16983.
[215] D. Kim et al., Nat. Nanotechnol. 13 (2018) 812–818.
[216] H. Sun et al., ACS Nano 8 (2014) 6202–6210.
[217] H.-Y. Lin et al., Chem. Eng. J. 411 (2021) 128469.
[218] X. Li et al., Adv. Funct. Mater. 25 (2015) 4929–4947.
[219] J.K. Kim et al., ACS Nano 7 (2013) 7207–7212.
[220] Y.-Q. Zhang et al., Nano Energy 2 (2013) 545–552.
[221] N. Gao et al., J. Appl. Polym. Sci. 137 (2020) 48443.
[222] F. Xie et al., J. Mater. Chem. A 7 (2019) 27567–27575.
[223] Y. Fu et al., Nat. Commun. 11 (2020) 845.

[224] C. Ma et al., Adv. Sci. 5 (2018) 1700996.
[225] S. Li et al., Energy Storage Mater. 32 (2020) 306–319.
[226] P. Ge et al., Adv. Sci. 5 (2018) 1800080.
[227] Y. Wang et al., Nat. Commun. 11 (2020) 2531.
[228] K.-H. Ye et al., Energy Environ. Sci. 10 (2017) 772–779.
[229] Y. Cui et al., Chem. Eng. J. (2021) 129595.
[230] Q. Li et al., J. Am. Chem. Soc. 134 (2012) 18932–18935.
[231] W. Li et al., Adv. Mater. 30 (2018) 1800676.
[232] J. Liu et al., Science 347 (2015) 970–974.
[233] J. Chen et al., ACS Appl. Mater. Interfaces 9 (2017) 18429–18433.
[234] K. Jiang et al., Adv. Mater. 30 (2018) 1800783.
[235] Z.-B. Qu et al., Angew. Chem., Int. Ed. 59 (2020) 8542–8551.
[236] J. Zhang et al., Angew. Chem., Int. Ed. 58 (2019) 9871–9875.
[237] D.L. Zhao et al., Water Res. 147 (2018) 43–49.
[238] C. Yang et al., Nat. Commun. 11 (2020) 1379.
[239] H.A. Nguyen et al., Proc. Natl. Acad. Sci. USA 118 (2021) e2023083118.